공학석사 학위 논문

Analysis and Tuning of Micro-Ring Structure including Mass Imperfections

질량 불완전성을 포함한 마이크로 링의 분석 및 조정

2023년 8월

서울대학교 대학원

항공우주공학과

김 기 윤

질량 불완전성을 포함한 마이크로 링의 분석 및 조정

Analysis and Tuning of Micro-Ring Structure including Mass Imperfections

지도 교수 김 지 환

이 논문을 공학석사 학위논문으로 제출함

2023년 8월

서울대학교 대학원
항공우주공학과
김 기 윤

김기윤의 공학석사 학위논문을 인준함
2023년 8월

Chair _____(Seal)
Vice Chair _____(Seal)
Examiner _____(Seal)

Abstract

Contrary to the theoretical concept, many structural models are often unstable due to structural flaws. Especially, some of flaws have a significant effect on the aerospace structure. Thus, it is necessary to analyze vibration analysis of imperfect ring. In the circumstance of structural flaws, the natural frequency of structure is divided with higher frequency and lower frequency. This paper explains to imperfect ring by using perturbation compared to simple theory assumed that the mode shape of imperfect ring is identical to perfect ring. Compared to simple theory, perturbation also deals with how to solve mode shapes as wells as natural frequencies by applying fourier series and it explains the variance of natural frequency and mode shape by mass imperfection. Besides this paper discusses thermo-elastic damping effect (TED) which is the key to derive Quality factor (Q-factor) and rotating ring. To easily express equation of motion, the rotating ring is considered by in-extensional assumption which is related to tangential displacement and radial displacement and linearization in perturbation. In case study, natural frequency, mode shape and Q-factor are investigated with the magnitude and location of imperfect mass and rotational speed by diverse method in macro-ring and micro-ring. Finally, this paper

suggests tuning method for reducing higher frequency and lower frequency which is showed by splitting of mass imperfection. To match frequency of the perfect ring, it proposes how to find the magnitude and location of adding or removing point masses.

Keyword : mass imperfection, splitting, tuning, TED, Q-factor, rotating

Student Number : 2021-26006

Table of Contents

List of Tables and Figures

Tables

Figures

List of Nomenclature

R	Radius
b	Height
h	Radial thickness
E	Young's modulus
I	Moment of inertia
A	Cross-sectional area
ρ	Density
M_θ	Moment resultant
N_θ	Force resultant
u	Radial coordinate
v	Circumferential coordinate
n	Mode number
k	Fourier coefficient
Ω	Rotating speed
ω_{0n}	Perfect frequency
ω_{nS}	Split frequency, S=H (higher), L (lower)
φ_n	Phase orientation
ψ	Test function
$\delta\rho(\theta)$	Imperfect density
$\delta\omega_n(\theta)$	Perturbed frequency by imperfection
$\delta u_n(\theta)$	Harmonic distortion by imperfection
T_a	Ambient temperature

α	Thermal expansion coefficient
C_v	Heat capacity per unit volume
χ	Thermal diffusivity
Π	The ratio of rotating speed and perfect frequency

1. Introduction

Many structures are theoretically designed and perfect. However, it is difficult to manufacture perfectly because of imperfections. To predict results by imperfection, it is necessary to consider structure combining imperfections such as point masses, stiffness. Some imperfections give the effects of frequency, mode shape and Q-factor in micro ring. Many researchers studied the vibration of structure and suggested many methods to solve problem.

Soedel [1] investigated rotating classical ring assumed to in-extension. He [2] also investigated natural frequencies and mode shapes in non-axisymmetric tire by applying receptance method which is used to action and reaction of structure and point mass. Bert [3] studied curved beam and shear deformable ring. Furthermore, He investigated the frequency and mode shape in non-axisymmetric tire which is non-uniformity configuration using the receptance method [4]. Since disadvantage of receptance method is to be difficult to calculate to some variable and external environment, Fox explained how to easily solve it using simple theory [5]. Simple theory is used to calculate the splitting frequency which occurs in slightly imperfect axisymmetric bodies. Compared to receptance method, simple theory has restriction to use to the

ring model such as small imperfection and in-extension. Lee [6] researched to predict the effects of local deviations which is based on the laplace transformation method and heavy-side unit step function. Using Local deviation, the natural frequencies and mode shapes of the ring are predicted for the point mass, sharp decrease in stiffness. Amabili [7] used receptance method to apply to the research of the free vibrations of cylindrical shell that was either empty or filled. Considering density of free and filled in cylindrical, he calculated natural frequency and mode shapes. Park [8] investigated structural dynamics modifications based on frequency response function to obtain optimal structural changes to improve natural frequencies. The optimal structural modification is calculated by combining eigenvalue sensitivities and eigenvalue reanalysis technique. Fox [9] studied when the ring model is connected to different types of random mass imperfections, how the natural frequency splits statistically. Bisegma [10] suggested perturbation method different simple theory. Perturbation method considers mode shapes as well as natural frequencies resulting from imperfect mass and stiffness compared to simple theory which is assumed that mode shape of imperfect ring is identical to perfect ring. Kim [11] explained strategy of asymmetric ring due to imperfect mass. He studied clear beats with proper periods in the first and the second

vibration modes by giving an example of Korean bell. Park [12] extensively examined the effect of multiple local deviations on the property of mode pair of ring and bell type structures such as circular ring, Korean bell using local deviation, [6]. Thao [13] researched natural frequencies of a clamped-clamped beam with concentrated masses calculated by receptance method which was based on theoretically exact. Chang [14] studied frequency derived by receptance method which is coupling of subsystems such as point masses, grounded springs, or spring-mass oscillators.

Q-factor is important factor in micro structure. Q-factor is even considered as variable of design. Zener [15] analyzed local fluctuations within a vibrating solid structure resulting from internal friction by heat conduction effects. Lifshitz and Roukes [16] investigated TED as a dissipation mechanism in micro and nano mechanical systems. Guo and Rogerson [17] studied the effect of thermoelastic coupling on a micro-machined resonator. Wong [18] investigated the application of Zener's theory to thin, circular rings. He also suggested a simple expression for the Q-factor associated with in-plane flexural modes of vibration. Furthermore, Wong and Fox [19] studied thermoealstic damping of the in-plane vibration of ring to gain advanced expression of energy-dissipation effects in MEMS resonators. Mioduchowski [20] examined Q-factor which is

considered by the effects of hollow geometry on thermoelastic dissipation of tubular beam resonators of circular corss-section. Hu [21] calculated frequencies and Q-factor of beam with mass and network of suspension. Pei [22] investigated Q-factor of rotating flexible annular micro-disk under thermoelastic coupling. Pawaskar [23] studied analytical solution for Q-factor in Timoshenko beam theory. Kim [24] studied Q-factor of ring with irregular mass and stiffness by using multi-deviation. Kim [25] also studied thermoelastic damping effect of rotating thin ring assumed to in-extensional vibration. Furthermore, Kim [26] examined natural frequency and Q-factor of imperfect rotating ring by point mass. Kim [27] examined Q-factor divided by higher mode and lower mode due to imperfection of mass. Kim [28] investigated Q-factor of toroidal micro ring which splits higher mode and lower mode by imperfect mass. Using receptance method of cylindrical shell [7], Kim [29] applied thermoelastic damping effect and Q-factor to imperfect cylindrical shell by mass.

Trimming (Tuning) is crucial to eliminate higher and lower frequencies as well as Q-factor by removing or adding point mass. In this regards, it is necessary to calculate the process of split in reverse. Rourke and William and Fox [30], [31] studied how to trim imperfect ring due to point mass by using inverse process. Wu [32]

investigated trimmed Q-factor of the trimmed resonator for the vibratory cupped gyroscopes. Tanaka [33] studied and examined Q-factor of multi ring in which the trimming location is chosen to independently modify the Q-factors of each axis.

The objective of this paper is to derive solution for imperfect rotating ring and calculate natural frequency and Q-factor as well as mode shape which cannot be calculated in simple theory. By developing inverse problem of split frequency and Q-factor, this paper suggests how to tune frequency and Q-factor of imperfect ring by removing or adding point mass.

2. Formulation

The rotating ring with rectangular cross-section is depicted in Fig.1 including arbitrary attached point masses. In this figure, R, b and h are mean radius, height and radial thickness of the model, respectively. In addition, As the ring model, isothermal Young's modulus, moment of inertia, cross-sectional area are defined as $E, I = bh^3/12$ and $A = bh$, respectively. The global polar coordinate system is used to describe the circumferential strain with local coordinate system. Especially, to show imperfection of masses, density with respect to the angular position is expressed as $\rho = \rho(\theta)$.

2.1. Equation of Motion in perfect rotating ring

Equation of motion for rotating thin rings are given as [1]

$$\frac{1}{R}\frac{\partial N_\theta}{\partial \theta} + \frac{1}{R^2}\frac{\partial M_\theta}{\partial \theta} - \rho A\left(\frac{\partial^2 u}{\partial t^2} + 2\Omega\frac{\partial v}{\partial t} - \Omega^2 u\right) = 0 \qquad (1.a)$$

$$\frac{1}{R}\frac{\partial^2 M_\theta}{\partial \theta^2} - \frac{N_\theta}{R} - \rho A\left(\frac{\partial^2 v}{\partial t^2} - 2\Omega\frac{\partial u}{\partial t} - \Omega^2(R+v)\right) = 0 \qquad (2.b)$$

where M_θ , N_θ present moment resultant, force resultant, respectively.

To eliminate radial strain, u for deriving easily, it is assumed that the ring is axially inextensible so that $v = -\partial u/\partial\theta$,

$$\varepsilon = \frac{1}{R}\left(\frac{\partial u}{\partial \theta} + v\right) = 0 \tag{3}$$

And the bending moment results on the cross-section of the model as ref. [1] is

$$M_\theta = \int_A (r\sigma_\theta) dA = \int_{-\frac{h}{2}}^{\frac{h}{2}} (r\sigma_\theta) b dr \tag{4}$$

Later, it is replaced to the bending moment with for explaining Thermal-elastic damping effect and Quality factor.

So eq. (4) is changed

$$M_\theta = -\frac{EI}{R^2}\left(\frac{\partial^2 u}{\partial \theta^2} + u\right) \tag{5}$$

Thus the equation of motion of the rotating ring is represented as

$$EI\left(\frac{\partial}{\partial\theta}+\frac{\partial^3}{\partial\theta^3}\right)\left(\frac{\partial v}{\partial\theta}+\frac{\partial^3 v}{\partial\theta^3}\right)$$
$$+\rho(\theta)AR^4\left[\frac{\partial^4 v}{\partial\theta^2\partial t^2}-\frac{\partial^2 v}{\partial t^2}+4\Omega\frac{\partial^2 v}{\partial\theta\partial t}-\Omega^2\left(\frac{\partial^2 v}{\partial\theta^2}-v\right)\right]=0 \tag{6}$$

As it is applied by harmonic vibration,

$$v(\theta,t)=v(\theta)e^{i\omega t} \tag{7}$$

where $v(\theta)$ denotes the vibration amplitude, substituting into Eq. (6), thus,

$$\left[EI\left(\frac{\partial}{\partial\theta}+\frac{\partial^3}{\partial\theta^3}\right)\left(\frac{\partial v}{\partial\theta}+\frac{\partial^3 v}{\partial\theta^3}\right)\right]$$
$$+\rho(\theta)AR^4\left[-\omega^2(\Omega)\left(\frac{\partial^2 v}{\partial\theta^2}-v\right)+4i\omega(\Omega)\Omega\frac{\partial v}{\partial\theta}\right. \tag{8}$$
$$\left.-\Omega^2\left(\frac{\partial^2 v}{\partial\theta^2}-v\right)\right]=0$$

where the subscripts n, Ω and $\omega(\Omega)$ represent rotating condition, mode number and the natural frequency of the ring.

2.1.1 Perfect Ring

If the perfect ring is perfect, the density of the ring, ρ, is independent of angular position, θ. i.e., it is denoted ρ_0. The function $v(\theta)$ is also denoted by $v_0(\theta)$. And because of in-extensible assumption as eq. (3), $v_{0n}(\theta)$ can be expressed as ref. [10].

$u_{0n}(\theta)$ is expressed

$$u_{0n}(\theta) = 2A_{0,n}\cos(n\theta + \varphi_n) = U_{0,n}e^{in\theta} + U_{0,-n}e^{-in\theta} \tag{9}$$

$$\begin{aligned} v_{0n}(\theta) &= -\frac{\partial u_{0n}(\theta)}{\partial \theta} = -2nA_{0,n}\sin(n\theta + \varphi_n) \\ &= inU_{0,n}e^{in\theta} - inU_{0,n}e^{-in\theta} \end{aligned} \tag{10}$$

$$U_{0,n} = A_{0,n}e^{i\varphi_n}, U_{0,-n} = \overline{U}_{0,n} \tag{11}$$

an overline denotes the complex conjugate, and A_{0n} is set in the natural number. The eigenmode $u_{0n}(\theta)$ is known as nth modal shape, and φ_n is its phase orientation. It is recalled that for every $n \geq 1$, two independent eigenmodes u_{0n} exist, corresponding to the same eigenfrequency ω_{0n} : hence, they are referred to as degenerate eigenmodes.

In the perfect ring, the natural frequency is the same whether the

equation of the ring is derived by perturbation method or simple theory. According to forward and backward rotational speed, Ω, the frequencies are divided by higher (asymmetric) mode, lower (symmetric) mode. To find the natural frequency of the perfect ring, the displacement v_{0n} in Eq. (10) can be substituted into Eq. (8), then the natural frequency of the rotating perfect ring is obtained as

$$\omega_{0n}(\Omega) = \frac{2\Omega n}{1+n^2} \pm \sqrt{\frac{EI}{\rho_0 A R^4}\frac{n^2(1-n^2)^2}{1+n^2} + \left(\frac{2\Omega n}{1+n^2}\right)^2 - \Omega^2} \qquad (12)$$

For $n = 0$, Only one independent eigenmode exists. The eigenmodes relevant to $n = 0$ and 1 correspond to rigid motions of the ring, and their eigenfrequencies are zero. In the following, the eigenmodes with $n \geq 2$ will be examined. They have nonzero eigenfrequencies and results in deformations of the ring, so that they are known as elastic eigenmodes. The natural frequency is if the flawless ring is not rotating.

$$\omega_{0n}(0) = \sqrt{\frac{EI}{\rho_0 A R^4}\frac{n^2(1-n^2)^2}{1+n^2}} \qquad (13)$$

2.1.2 Imperfect Ring

The coinciding frequency, eq. (12), relevant to couples of degenerate eigenmodes, eq. (10), splits into two distinct values as well as the rotational orientation despite the addition of a minor amount of mass imperfection to a perfect ring. Moreover, their corresponding eigenmodes deviate from the sinusoidal shape, eq. (9).

This section presents a model that leads to analytical expression of the eigenfrequencies and modal structures of an imperfect ring under a general imperfect condition. To solve an imperfect ring with point masses, it is necessary to include the test function, ψ in the formulation for the weak form.

$$\psi = e^{-ik\theta} \tag{14}$$

A weak formulation becomes

$$\begin{aligned}\int_0^{2\pi}\left[\frac{EI}{AR^4}\left(\frac{\partial}{\partial\theta}+\frac{\partial^3}{\partial\theta^3}\right)\left(\frac{\partial v}{\partial\theta}+\frac{\partial^3 v}{\partial\theta^3}\right)\right]\psi\, Rd\theta \\ +\int_0^{2\pi}\rho(\theta)\psi\left[-\omega^2(\Omega)\left(\frac{\partial^2 v}{\partial\theta^2}-v\right)+4i\omega(\Omega)\Omega\frac{\partial v}{\partial\theta}\right. \\ \left.-\Omega^2\left(\frac{\partial^2 v}{\partial\theta^2}-v\right)\right]Rd\theta = 0\end{aligned} \tag{15}$$

By partial derivation, eq. (15) is replaced as

$$
\begin{aligned}
&-\int_0^{2\pi}\left[\frac{EI}{AR^4}\left(\frac{\partial\psi}{\partial\theta}+\frac{\partial^3\psi}{\partial\theta^3}\right)\left(\frac{\partial v}{\partial\theta}+\frac{\partial^3 v}{\partial\theta^3}\right)\right]Rd\theta \\
&-\int_0^{2\pi}\rho(\theta)\left[\omega^2(\Omega)\left(v\psi+\frac{\partial v}{\partial\theta}\frac{\partial\psi}{\partial\theta}\right)-2i\omega(\Omega)\Omega\left(\frac{\partial v}{\partial\theta}\psi+v\frac{\partial\psi}{\partial\theta}\right)\right. \\
&\qquad\left.+\Omega^2\left(v\psi+\frac{\partial v}{\partial\theta}\frac{\partial\psi}{\partial\theta}\right)\right]Rd\theta=0
\end{aligned}
\tag{16}
$$

The imperfect of mass density is accounted for as follow :

$$\rho(\theta)=\rho_0+\delta\rho(\theta) \tag{17}$$

where $\delta\rho(\theta)$ represents $2\pi-$periodic perturbations of the perfect ring's mass densityρ_0. Accordingly, the eigenmodes $u_n(\theta)$ and the corresponding eigenfrequencies $\omega_n(\Omega)$ of the imperfect ring are represented as

$$\omega_n(\Omega)=\omega_{0n}(\Omega)+\delta\omega_n(\Omega) \tag{18}$$

$$v_n(\theta)=v_{0n}(\theta)+\delta v_n(\theta) \tag{19}$$

where $\delta u_n(\theta)$, here denoted as "harmonic distortion", is an undetermined perturbation of the modal shape $u_{0n}(\theta)$ of the perfect

ring, which accounts for the vibration localization and rotational speed in ref. [10]. The unknown shift of the correspond modal eigenfrequency is denoted by $\delta\omega_n(\Omega)$.

By substituting eqs. (17), (18) and (19) into Eq. (16), it is presented as :

$$
\begin{aligned}
&-\int_0^{2\pi}\left[\frac{EI}{AR^4}\left(\frac{\partial\psi}{\partial\theta}+\frac{\partial^3\psi}{\partial\theta^3}\right)\left(\frac{\partial(v_{0n}+\delta v_n)}{\partial\theta}\right.\right.\\
&\left.+\frac{\partial^3\big(v_{0n}(\theta)+\delta v_n(\theta)\big)}{\partial\theta^3}\right)\\
&+(\rho_0+\delta\rho)\left[\big(\omega_{0n}(\Omega)+\delta\omega_n(\Omega)\big)^2\left((v_{0n}+\delta v_n)\psi\right.\right.\\
&\left.+\frac{\partial(v_{0n}+\delta v_n)}{\partial\theta}\frac{\partial\psi}{\partial\theta}\right)\\
&-2i\big(\omega_{0n}(\Omega)+\delta\omega_n(\Omega)\big)\Omega\left(\frac{\partial(v_{0n}+\delta v_n)}{\partial\theta}\psi+(v_{0n}+\delta v_n)\frac{\partial\psi}{\partial\theta}\right)\\
&\left.\left.+\Omega^2\left((v_{0n}+\delta v_n)\psi+\frac{\partial(v_{0n}+\delta v_n)}{\partial\theta}\frac{\partial\psi}{\partial\theta}\right)\right]\right]Rd\theta=0
\end{aligned}
\tag{20}
$$

In order to derive closed-form expressions for the rotational modal frequency shift $\delta\omega_n(\Omega)$ and the harmonic distortion δu_n, a linearized version of eq. (20) is here derived. It is obtained by neglecting higher-order terms in eq. (20) :

$$\int_0^{2\pi} \frac{EI}{AR^4}\left(\frac{\partial \delta v_n}{\partial \theta}+\frac{\partial^3 \delta v_n}{\partial \theta^3}\right)\left(\frac{\partial \psi}{\partial \theta}+\frac{\partial^3 \psi}{\partial \theta^3}\right) Rd\theta$$

$$-\int_0^{2\pi} \left(\omega_{0n}^2(\Omega)\rho_0 - 2i\Omega\rho_0\omega_{0n}(\Omega)\right)\left(\delta v_n \psi + \frac{\partial \delta v_n}{\partial \theta}\frac{\partial \psi}{\partial \theta}\right) Rd\theta$$

$$=\int_0^{2\pi} (\omega_{0n}^2(\Omega)\delta\rho + 2\omega_{0n}(\Omega)\delta\omega_n(\Omega)\rho_0 + \Omega^2\delta\rho)\left(v_{0n}\psi \right. \tag{21}$$

$$\left. + \frac{\partial v_{0n}}{\partial \theta}\frac{\partial \psi}{\partial \theta}\right) Rd\theta$$

$$-\int_0^{2\pi} \left(2i\Omega\rho_0\delta\omega_n(\Omega) + 2i\Omega\delta\rho\omega_{0n}(\Omega)\right)\left(v_{0n}\frac{\partial \psi}{\partial \theta}+\frac{\partial v_{0n}}{\partial \theta}\psi\right) Rd\theta$$

The mass−density perturbation $\delta\rho(\theta)$ is depicted by the Fourier series expansion as Ref. [10]:

$$\delta\rho(\theta) = \sum_{k=-\infty}^{+\infty} \{\delta\rho\}_k \, e^{ik\theta} \tag{22}$$

where $\{c\}$ is the vector comprising the Fourier coefficients of a function $c(\theta)$, and $\{c\}_k$ is its kth component. Naturally, it turns out that $\{c\}_{-k} = \overline{\{c\}}_k$. Additionally, the unidentified harmonic distortion $\delta v_n(\theta)$ is represented by its Fourier series expansion. Because the ring is applied to an in−extensional assumption, $\delta v_n(\theta)$ can be replaced with $\delta u_n(\theta)$.

$$\delta v_n(\theta) = \sum_{k=-\infty}^{+\infty} \{\delta v_n\}_k \, e^{ik\theta} = -ik \sum_{k=-\infty}^{+\infty} \{\delta u_n\}_k \, e^{ik\theta} \tag{23}$$

As mentioned in Ref [10], we can infer, without loss of generality, that

$$\{\delta u_n\}_n = 0 \tag{24}$$

since the phase orientation φ_n is assumed as unknown quantity.

The Fourier series expansions, eqs. (22) and (23) are substituted in Eq. (21). The test function, ψ is taken as follows :

$$\psi = e^{-ik\theta}, k \in \mathbb{N} \tag{25}$$

After simple algebra, the following equation is obtained, for $k \in \mathbb{N}$ excepted $k = n$;

$$\begin{aligned} &\frac{\{\delta u_n\}_k}{A_{0n}} \left[\frac{1+k^2}{1+n^2} - \frac{k^2(1-k^2)^2}{n^2(1-n^2)^2} + \Pi^2 \frac{1+k^2}{1+n^2}\right] \\ &= -\frac{\{\delta\rho\}_{-n+k}}{\rho_0} e^{i\varphi_n} \left[\frac{n(1+nk)}{k(1+n^2)} + 2\Pi \frac{n(n-k)}{k(1+n^2)} + \Pi \frac{n(1+nk)}{k(1+n^2)}\right] \\ &+ \frac{\{\delta\rho\}_{n+k}}{\rho_0} e^{-i\varphi_n} \left[\frac{n(1-nk)}{k(1+n^2)} - 2\Pi \frac{n(n+k)}{k(1+n^2)} + \Pi^2 \frac{n(1-nk)}{k(1+n^2)}\right] \end{aligned} \tag{26}$$

where Π is rotating speed ratio, the rotating speed per perfect frequency, $\Pi = \Omega/\omega_{0n}$.

Eq.(26) yields the Fourier coefficients of the harmonic distortion δu_n.

Alternatively, the following equation is derived for $= n$:

$$0 = 2\frac{\delta\omega_n(\Omega)}{\omega_{0n}} - \frac{\{\delta\rho\}_0}{\rho_0}e^{i\varphi_n}[1+\Pi^2] + \frac{\{\delta\rho\}_{2n}}{\rho_0}\ e^{-i\varphi_n}\left[\frac{1-n^2}{1+n^2} - 4\Pi\frac{n}{1+n^2} + \Pi^2\frac{1-n^2}{1+n^2}\right] \tag{27}$$

This equation results in :

$$\frac{\delta\omega_n(\Omega)}{\omega_{0n}} = -\frac{1}{2}\frac{\{\delta\rho\}_0}{\rho_0}[1+\Pi^2] + \frac{1}{2}\ \frac{\{\delta\rho\}_{2n}}{\rho_0}\ e^{-2i\varphi_n}\left[\frac{1-n^2}{1+n^2} - 4\Pi\frac{n}{1+n^2} + \Pi^2\frac{1-n^2}{1+n^2}\right] \tag{28}$$

Since both the left−hand side and the first term on the right−hand side of the previous equation are real, the second term at the right−hand side must also be real. Consequently, it follows that :

$$\varphi_n = \frac{1}{2}\arg\left[\frac{1-n^2}{1+n^2} - 4\Pi\frac{n}{1+n^2} + \Pi^2\frac{1-n^2}{1+n^2}\right] + l\frac{\pi}{2} \tag{29}$$

where l present higher mode and lower mode, $l = 0,1$

Hence

$$\frac{\delta\omega_n(\Omega)}{\omega_{0n}(\Omega)} = -\frac{1}{2}\frac{\{\delta\rho\}_0}{\rho_0}[1+\Pi^2] \\ -\frac{(-1)^l}{2}\left|\frac{\{\delta\rho\}_{2n}}{\rho_0}\left[\frac{1-n^2}{1+n^2} - 4\Pi\frac{n}{1+n^2} + \Pi^2\frac{1-n^2}{1+n^2}\right]\right| \tag{30}$$

As expected, it turns out that for each elastic modes, $n \geq 2$, there are two separate frequencies each with a higher frequency and a lower frequency. Therefore, the mode n relevant frequency split (or mistuning) comes out to be

$$\frac{\Delta\delta\omega_n(\Omega)}{\omega_{0n}(\Omega)} = \left[\frac{1-n^2}{1+n^2} - 4\Pi\frac{n}{1+n^2} + \Pi^2\frac{1-n^2}{1+n^2}\right]\left|\frac{\{\delta\rho\}_{2n}}{\rho_0}\right| \tag{31}$$

2.1.3 Point masses added to the ring

In case of p point masses m_j located in the ring at the angular positions $\theta = \Theta_j$, imperfection due to point masses is presented as

$$\delta\rho(\theta) = \sum_{j=1}^{p} \frac{m_j}{R} \boldsymbol{\delta_\theta}(\Theta_j) \tag{32}$$

where $\delta_\theta(\Theta_j)$ denotes the Dirac delta function supported at Θ_j. The Fourier coefficients of the mass density perturbation $\delta\rho$ are given by

$$\{\delta\rho\}_k = \sum_{j=1}^{p} \frac{m_j}{2\pi R} e^{-ik\Theta_j} \tag{33}$$

The phase orientation $\varphi_{n,l}$, eq. (29) yields

$$\varphi_{n,l} = -\frac{1}{2}\arctan\frac{\sum_{j=1}^{p} m_j \sin 2n\Theta_j}{\sum_{j=1}^{p} m_j \cos 2n\Theta_j} + l\frac{\pi}{2}, \qquad l = 0,1 \tag{34}$$

from eq. (30) it turns out that

$$\frac{\delta\omega_n(\Omega)}{\omega_{0n}} = -\frac{1}{2}M_0\left([1+\Pi^2]\sum_{j=1}^{p} m_j - (-1)^l \left[\frac{1-n^2}{1+n^2} - 4\Pi\frac{n}{1+n^2} + \Pi^2\frac{1-n^2}{1+n^2}\right] \left| \sum_{j=1}^{p} m_j\, e^{-2in\Theta_j} \right| \right) \tag{35}$$

where $M_0 = 2\pi R\rho_0$ is the mass of the perfect ring.

Expression of the phase orientation $\varphi_{n,l}$, eq. (34) is equivalent to

expression (7) of $\psi_{n,l}$ derived in Ref. [5], by noting that $\psi_{n,l} = -\varphi_{n,l}/n$.

Finally, from Eq. (26), for $k \neq n$, the Fourier coefficients of $\delta u_{n,l}$ are obtained :

$$
\begin{aligned}
&\frac{\{\delta u_n\}_k}{A_{0n}} \\
&= -\frac{1}{\left[\frac{1+k^2}{1+n^2} - \frac{k^2(1-k^2)^2}{n^2(1-n^2)^2} + \Pi^2 \frac{1+k^2}{1+n^2}\right]} \\
&\left(\frac{\sum_{j=1}^{p} m_j}{M} e^{i\{(-n+k)\theta+\varphi_n\}} \left[\frac{n(1+nk)}{k(1+n^2)} + 2\Pi \frac{n(n-k)}{k(1+n^2)}\right.\right. \\
&\left. + \Pi \frac{n(1+nk)}{k(1+n^2)}\right] \\
&+ \frac{\sum_{j=1}^{p} m_j}{M} e^{-i\{(n+k)\theta+\varphi_n\}} \left[\frac{n(1-nk)}{k(1+n^2)} - 2\Pi \frac{n(n+k)}{k(1+n^2)}\right. \\
&\left.\left. + \Pi^2 \frac{n(1-nk)}{k(1+n^2)}\right]\right)
\end{aligned}
\tag{36}
$$

with $\varphi_{n,l}$ given in Eq. (34).

In order to investigate the vibration phenomenon due to the imperfect of mass, the total harmonic distortion (THD) index is introduced for each split eigenmode in ref [10]:

$$THD = \frac{\|\delta u_{n,l}\|_2}{\|u_{0n}\|_2} = \sqrt{\frac{\sum_{k=-\infty}^{+\infty} \left|\{\delta u_{n,l}\}_k\right|^2}{2A_{0n}^2}} \tag{37}$$

This index measures the contribution of mode shape by imperfection difference from the fundamental u_{0n} to the modal shape $u_{n,l}$ of the imperfect ring.

2.2. Thermo-elastic damping effect

In general, the energy conversion relationship between strain $\varepsilon = \varepsilon_r + \varepsilon_\theta + \varepsilon_z$ and thermal energies yields TED effect. Then the Fourier equation for heat conduction is appropriate for determining the relationship. The heat conduction equation is utilized to obtain the temperature profile for the thermal flux in conjunction with the strain.

$$\frac{\partial T}{\partial t} - \chi \nabla^2 T = -\frac{E\alpha T_a}{C_v(1-2v)}\left(\frac{\partial \varepsilon}{\partial t}\right) \tag{38}$$

where $T = T(r,\theta,z,t) = T_0(r,\theta,z)e^{i\omega t}$ is the difference of the temperature from the ambient temperature T_a. Furthermore, α, χ, C_v

and ν are thermal expansion coefficient, thermal diffusivity, heat capacity per unit volume and Poisson's ratio of the material, respectively.

To express TED in micro-ring structure as displacement and thermal terms, the components of strain with thermal effect can be written as

$$\varepsilon_\theta = \frac{1}{E}\sigma_\theta + \alpha T \tag{39}$$

$$\varepsilon_r = \varepsilon_z = -\frac{\mu}{E}\sigma_\theta + \alpha T \tag{40}$$

$$\sigma_\theta = E(\varepsilon_\theta - \alpha T) \tag{41}$$

In order to determine the temperature profile of the ring structure, Eqs. (39)-(41) are substituted into Eq. (38) by the process in Ref. [19] with approximation such as $1+\mu \approx 1$ and $R+r \approx R$. As the boundary condition, there is no heat flux at both edges of the radial thickness. Then the heat conduction equation can be simplified into one-dimensional as

$$\frac{\partial^2 T}{\partial \theta^2} - \frac{1}{\chi}\frac{\partial T}{\partial \theta} = -\frac{1}{\chi}\frac{\Delta_E}{\alpha}\frac{\partial}{\partial \theta}\left[\frac{r}{R}\left(\frac{\partial^2 u}{\partial \theta^2} + u\right)\right] \tag{42}$$

where $\Delta_E = E\alpha^2 T_a / C_v$ is defined as the relaxation strength of the Young's modulus.

As in Ref [19], the solution of the temperature profile is obtained as

$$T_0(x,\theta) = \frac{\Delta_E}{\alpha}\frac{1}{R^2}\left(\frac{\partial^2 u}{\partial\theta^2} + u\right)\left(x - \frac{\sin kx}{k\cos\frac{kh}{2}}\right) \tag{43}$$

where $k = k(\omega) = (1-i)\sqrt{\frac{\omega}{2\chi}}$.

Furthermore, the bending moment resultant on the cross-section of the model with thermal effect (5) is replaced in ref [19]

$$M_\theta = -\frac{E_\omega I}{R^2}\left(\frac{\partial^2 u}{\partial\theta^2} + u\right) = -\frac{E[1+\Delta_E\{1+f(\omega)\}]I}{R^2}\left(\frac{\partial^2 u}{\partial\theta^2} + u\right) \tag{44}$$

where E_ω is Young's modulus with TED according to the natural frequency with

$$f(\omega) = \frac{24}{k^3h^3} = \left[\left(\frac{kh}{2}\right) - \tan\left(\frac{kh}{2}\right)\right] \tag{45}$$

By applying TED, equations to frequency and mode shape in macro ring, eq. (35) and eq. (36) are changed :

$$\frac{\delta\omega_n(\Omega)}{\omega_{0n}} = -\frac{1}{2}M_0\left(\left[1+\Pi^{*2}\right]\sum_{j=1}^{p} m_j - (-1)^l\left[\frac{1-n^2}{1+n^2} - 4\Pi^*\frac{n}{1+n^2} + \Pi^{*2}\frac{1-n^2}{1+n^2}\right]\left|\sum_{j=1}^{p} m_j\, e^{-2in\Theta_j}\right|\right) \tag{46}$$

$$\frac{\{\delta u_n\}_k}{A_{0n}} = -\frac{1}{\left[\frac{1+k^2}{1+n^2} - \frac{k^2(1-k^2)^2}{n^2(1-n^2)^2} + \Pi^{*2}\frac{1+k^2}{1+n^2}\right]} \left(\frac{\{\delta\rho\}_{-n+k}}{\rho_0} e^{i\varphi_n}\left[\frac{n(1+nk)}{k(1+n^2)} + 2\Pi^*\frac{n(n-k)}{k(1+n^2)} + \Pi^*\frac{n(1+nk)}{k(1+n^2)}\right] + \frac{\{\delta\rho\}_{n+k}}{\rho_0} e^{-i\varphi_n}\left[\frac{n(1-nk)}{k(1+n^2)} - 2\Pi^*\frac{n(n+k)}{k(1+n^2)} + \Pi^{*2}\frac{n(1-nk)}{k(1+n^2)}\right]\right) \tag{47}$$

where Π^* means the ratio of rotating speed and combination of perfect frequency applied TED and without TED, $\Pi^* = \Omega/\{\omega_{0n}^*(\Omega)\omega_{0n}(\Omega)\}$.

Finally, TED effect on the rotating micro-ring with imperfection is expressed as the ratio of dissipated energy, defined by Q-factor.

The general definition of Q is given as

$$Q = \frac{1}{2}\left|\frac{Re\left(\omega_{ns}^{*}(\Omega)\right)}{Im\left(\omega_{ns}^{*}(\Omega)\right)}\right| = \frac{1}{2}\left|\frac{Re\left(\omega_{0n}^{*}(\Omega) + \delta\omega_{nS}^{*}(\Omega)\right)}{Im\left(\omega_{0n}^{*}(\Omega) + \delta\omega_{nS}^{*}(\Omega)\right)}\right| \quad (48)$$

Compared to THD of macro ring, THD is calculated by perfect frequency with TED in micro ring.

2.3. Tuning of ring

Tuning of frequency in imperfect ring is inverse problem. In the case of non-rotating, the trimming method is explained in ref [30] and Ref [31]. This section explains how to solve the trimming method when rotating a defective ring in a macro-ring and micro-ring with TED.

The objective of tuning is to eliminate the gap of higher and lower frequencies by removing or adding a suitable continuous mass distribution $\delta\rho_{tr}(\theta)$ to the ring. To do this, it is necessary to calculate proper the magnitude and location of trimming mass through inverse process. by adding a suitable continuous mass distribution $\delta\rho_{tr}(\theta)$ to the ring.

In order to acquire trimming, as a first step, it is necessary to experimentally characterize the imperfect ring.

Thus it should find the difference of frequency in higher mode and lower mode.

The difference of higher and lower frequencies of imperfect rotating ring in eq. (31) :

$$\begin{aligned}\Delta\omega_n(\Omega) &= [\omega_{0n}(\Omega) + \delta\omega_{nH}(\Omega)] - [\omega_{0n}(\Omega) + \delta\omega_{nL}(\Omega)] \\ &= \delta\omega_{nH}(\Omega) - \delta\omega_{nL}(\Omega)\end{aligned} \tag{49}$$

This is the modal split (mistuning).

Following ref. [10], the trimming procedure here adopted hinges on determining a continuous mass distribution $\delta\rho_{sp}(\theta)$, which if added to a perfect ring, which coincide with the corresponding measured quantities $\Delta\omega_n(\Omega)$ and φ_n, respectively. Hence the mass distribution $\delta\rho_{sp}(\theta)$, according to eq. (34) and eq. (35) must satisfy the equations :

$$\Delta\delta\omega_n(\Omega) = \omega_{0n}(\Omega)\left[\frac{1-n^2}{1+n^2} - 4\Pi\frac{n}{1+n^2} + \Pi^2\frac{1-n^2}{1+n^2}\right]\left|\frac{\{\delta\rho_{split}\}_{2n}}{\rho_0}\right| \tag{50}$$

$$\varphi_{n,split} = \frac{1}{2}\ \arg\left[\left(\frac{1-n^2}{1+n^2} - 4\Pi\frac{n}{1+n^2} + \Pi^2\frac{1-n^2}{1+n^2}\right)\frac{\{\delta\rho_{sp}\}_{2n}}{\rho_0}\right] \tag{51}$$

which yields

$$\{\delta\rho_{split}\}_{2n} = \rho_0 \left(\frac{1-n^2}{1+n^2} - 4\Pi\frac{n}{1+n^2} + \Pi^2\frac{1-n^2}{1+n^2}\right)\frac{\Delta\omega_n(\Omega)}{\omega_{0n}(\Omega)}e^{2i\varphi_n} \qquad (52)$$

Consequently, any continuous mass distribution $\delta\rho_{split}(\theta)$ whose Fourier coefficients $\{\delta\rho_{split}\}_{2n}$ are given by Eq. (52), produces the calculated modal mistuning $\Delta\omega_{n,split}(\Omega)$ and phase orientation $\varphi_{n,split}$, when $\delta\rho_{split}(\theta)$ is given to the perfect ring with any such continuous mass distribution. According to Eq. (50), it turns out that the eigenfrequency $\omega_{0n}(\Omega)$ of perfect ring coincides with the average of the eigenfrequencies $\omega_{nH}(\Omega)$ and $\omega_{nL}(\Omega)$ of imperfect ring applied point masses, provided that $\delta\rho_{split}(\theta)$ is chosen with null average (i.e., $\{\delta\rho_{split}\}_0 = 0$). As a result, $\omega_{0n}(\Omega)$ could be identified with the average of the experimentally measured eigenfrequencies.

The modes n of the imperfect ring can be trimmed by the linear model, by simply adding any continuous mass distribution $\delta\rho_{tr}(\theta)$. This suggests that such a mass distribution $\delta\rho_{tr}(\theta)$ could trim also the real imperfect ring.

An simple way to obtain distribution of continuous mass is to sample the function $\delta\rho_{tr}(\theta)$ at N equi-spaced locations : i.e., at the angles

$$\theta_{l,tr} = \theta_0 + l\theta_s, \qquad l = 0 \cdots N-1 \qquad (53)$$

where θ_0 is an arbitrary initial sampling angle and $\theta_s = 2\pi/N$ is the angular sampling period. Setting $n_{max} = \max N$, and observing that the spectrum of the function $\delta\rho_{tr}(\theta)$ contains spatial circular frequencies up to $2n_{max}$, according to the Nyquist theorem, it must result :

$$\frac{2\pi}{\theta_s} = N > 2(2n_{max}) = 4n_{max} \tag{54}$$

At Eq. (53), $\delta\rho_{tr}(\theta)$ could be also chosen that such that its Fourier coefficients different from those cited above is zero : accordingly, such a continuous distribution is

$$\{\delta\rho_{split}\}_{2n} = \rho_0 \frac{1}{\frac{1-n^2}{1+n^2} - 4\Pi\frac{n}{1+n^2} + \Pi^2\frac{1-n^2}{1+n^2}} \frac{\Delta\omega_n(\Omega)}{\omega_{0n}(\Omega)} e^{2i\varphi_n} \tag{55}$$

Accordingly, the continuous mass distribution give in Eq. (55) is replaced by the sampled one :

$$\delta\rho_{tr,s}(\theta) = \frac{2\pi}{N}\sum_{l=0}^{N-1} \delta\rho_{tr}(\theta_{l,tr})\,\boldsymbol{\delta}_{\boldsymbol{\theta}_{l,tr}}(\theta) \tag{56}$$

The sampled mass distribution given in Eq. (56) corresponds to the following trimming masses :

$$m_{l,tr} = \frac{2\pi R}{N}\delta\rho_{tr}(\theta_{l,tr}), \qquad l = 0 \cdots N-1 \tag{57}$$

which recalling Eq. (52), can be calculated via the following explicit formula :

$$m_{l,tr} = M_0 \frac{1}{\frac{1-n^2}{1+n^2} - 4\Pi\frac{n}{1+n^2} + \Pi^2\frac{1-n^2}{1+n^2}} \frac{\Delta\omega_n(\Omega)}{\omega_{0n}(\Omega)}\cos 2\left(n\theta_{l,tr} + \varphi_{n,split}\right), \qquad l = 0 \cdots N-1 \tag{58}$$

If no target trimming is required, an arbitrary constant term may be added to the right hand side of eq. (58), i.e., each trimming mass $m_{l,tr}$ may be increased (or decreased) by the same arbitrary quantity, without modifying the achieved trimming condition. This freedom may be used, e.g., to have all trimming masses positive (or negative), if this situation is preferred for easiness of manufacturing. The Phase orientation, φ_n is different in higher mode and lower mode. But it is only used to higher mode in paper. Equation of tuning mass can be used to imperfect ring regardless of rotating, TED.

3. Results and Discussions

In this chapter, the frequency and mode shape of the imperfect rotating ring are investigated. Likewise, the complex frequency and Q-factor are also calculated. Also, this chapter also suggests how to change the mistuned frequencies and Q-factor of imperfect ring like a perfect ring by removing or adding mass (inverse problem). In addition, it investigates the change of mode shape and total harmonic distortion by trimming mass. In this paper, ring model is investigated with the structural parameter as in table 1 (a) in ref [10] and table 1 (b) in ref. [19]. And Table 2 also presents thermal parameter in ref. [19].

3.1. Code Verification

In this section, the perfect ring is selected to examine frequency and Q-factor under macro and micro size. Additionally, the split frequencies and Q-factor are calculated in imperfect ring with point mass.

Table 3 (a) and (b) present modal frequencies of perfect macro ring

and micro ring. Because of the size, the unit of modal frequency in macro ring is Hz, but the unit of micro ring is kHz. And the frequency result is greater the higher the mode number.

Table 4 (a) and (b) is modal frequencies of imperfect macro ring and micro ring with mass ratio, $m/M = 0.01$. higher frequencies by perturbation are same as simple theory but lower frequencies by perturbation are smaller than simple theory.

Fig 2. (a) and (b) present forward frequency and backward frequency in accordance with rotating speed ratio, Ω. There is a rotating speed ratio where forward frequency and backward frequency meet, which is the value before the imaginary value in eq. (30). In the backward rotating, there is a rotating ratio which is rotating, but its frequency is zero. This phenomenon is 'stationary condition' which means that the mode does not rotate with the rotating ring but appears as a stationary distortion of the ring to an observer who is not rotating with the ring as ref [1].

Table 5 (a), (b) and (c) present Q-factor of no rotating perfect ring. As the mode number increases, the Q-factor also increases such as frequency.

Fig. 3 is Q-factor in accordance with rotating speed ratio. Q-factor by forward increases as the rotating speed ratio increases, but decreases at some point. On the contrary, Q-factor by forward

decreases as rotating speed ratio, but increases at some point.

3.2. Natural frequency

In this section, it is investigated how the change of frequency derived by perturbation is calculated based on the rotating speed ratio and magnitude of mass in macro ring.

Fig 4. shows the difference of higher and lower frequencies in accordance with magnitude of mass. As the mass ratio increases, the difference of frequencies increases. Since the lower frequency by perturbation is less than simple theory, the difference of frequencies by perturbation is greater than simple theory.

Fig.5 shows the ratio of the difference of higher frequency and lower frequency in accordance with rotating speed ratio in macro ring at n=2. In forward rotating, the difference of higher and lower frequencies by perturbation increases, but the difference by simple theory has little difference and surges. In backward rotating, the differences of higher and lower frequencies by perturbation and simple theory have resonance.

3.3. Quality factor

In this section, Q-factor is investigated in accordance with rotating speed ratio and magnitude of mass.

Table 6 (a), (b) and (c) is the Q-factor dependent on rotating speed ratio, $\Omega/\omega_{0n} = 0$, $\Omega/\omega_{0n} = 0.5$, $\Omega/\omega_{0n} = 1$ at T=298K. In forward situation, higher Q-factor by perturbation is greater than simple theory but lower Q-factor by perturbation is less.

Fig. 6 (a), (b) and (c) shows the difference of higher Q-factor and lower Q-factor in accordance with mass ratio at n=2. The higher rotating speed ratio, the difference of Q-factor is greater.

Likewise, Fig. 7 (a), (b) and (c) shows Q-factor in accordance with rotating speed ratio at T=298K and n=2. As shown in Fig. 7, the rotating speed ratio has a big effect on Q-factor as well as frequency.

3.4. Mode shape

In this section, mode shape derived by perturbation is investigated in accordance with mass ratio and rotating speed ratio. Also total harmonic distortion, eq. (37), which means the change of mode shape by imperfect mass is investigated in the case of rotating

speed ratio and magnitude of mass.

Fig. 8 is mode shape of imperfect macro ring with 1% point mass and rotating speed ratio, $\Omega/\omega_{0n} = 1$.

Fig. 9 shows total harmonic distortion in accordance with mass ratio and rotating speed ratio. THD can be obtained when there is an imperfect mass in ring, when the mass ratio is zero, there is no THD value regardless of rotating speed ratio.

Fig. 10 shows THD in accordance with rotating speed ratio in macro ring with imperfect mass, $m/M = 0.01$. This figure is similar to Q-factor, fig. 7. And it has the value of rotating ratio which is similar to frequency, fig. 3.

Fig. 11 (a) and (b) show total harmonic distortion of higher mode and lower mode in accordance with mass ratio in macro ring at n=2. As mass ratio increases, THD generally increases. In backward rotating, THD in backward rotating totally is smaller than THD in no-rotating.

Fig. 12 is total harmonic distortion in accordance with rotating speed ratio in micro ring. THD in micro ring has no difference of temperature. In backward rotating, THD appears phenomenon such as resonance at specific result of rotating speed ratio. This reason is because the denominator of eq. (47) goes from zero at a certain rotating speed ratio value.

Fig. 13 is THD in accordance with mass ratio in micro ring. Similar to Fig. 11, THD of backward rotating is totally smaller than no-rotating. Because of size compared to macro ring, THD of forward rotating is greater than macro ring.

3.5. Tuning

This section explains how to calculate magnitude and location of trimming mass to eliminate higher and lower frequencies as well as Q-factor by removing or adding mass in ring model. Through inverse process, eqs(53)-(58) can get rid of difference of frequencies and Q-factor.

Before doing tuning, Fig. 14 (a), (b) and (c) show the difference of tuned frequency and perfect frequency Q-factor in accordance with mass ratio and tuning location at rotating speed ratio in macro ring. In here, if the gap of tuned frequency and perfect frequency is zero, this point is tuning point of magnitude and location of trimming mass. In the case of rotating speed ratio, $\Omega/\omega_{0n} = 1$, since lower frequency is resonance such as in fig. 5, it is not possible to compute tuning results.

Fig. 15 (a), (b) and (c) show the difference of tuned Q-factor and

perfect Q-factor in accordance with mass ratio and tuning location at rotating speed ratio in micro ring. If the gap of tuned Q-factor and perfect Q-factor is zero, this point is likewise tuning point of magnitude and location of trimming mass. As rotating speed ratio increases, the maximum of difference of tuned Q-factor and perfect Q-factor is increased.

Fig. 16 and Fig. 17 present the picture in which magnitude and location of trimming mass is suitable at n=2, n=3 using eq. (50)-(52). These positions is located to tune imperfect ring regardless of rotating.

4. Conclusion and future work

Although all structures are expected to be manufactured without flaws, there are sometimes imperfections such as mass, stiffness which result in frequency split and mistuning of structure.

In this work, analytical model for imperfect rectangular ring with thermo-elastic damping is investigated. This ring is based on the assumptions of in-extension and linearization. It shows the changes of frequency, q-factor and mode shape caused by imperfect mass using perturbation method in a spinning situation. Compared to simple theory, because perturbation method is assumed that frequency and mode shape split due to imperfection, perturbation method can show mode shape depending on the size of the ring, rotating speed ratio and imperfect mass. Thus, using the perturbation method, mistuned frequency and q-factor can be calculated more precisely from a rotating ring with an imperfect mass, and the mode shape can also be investigated in greater detail. The ring mistuned by point mass affects to whole system and results in split of natural frequencies and increase of the damping effect as well as mode shape.

In addition, the magnitude and location of the trimming mass are determined through the use of the inverse process to equalize the

split frequency and q-factor generated by an imperfect ring to a perfect ring. Through this procedure, it is expected that unbalanced ring can be tuned by removing or adding trimming mass.

As future works, studies will be investigated in a variety of situations. For examples, it can be studied in the case of non-linearity for improving the accuracy of frequencies and mode shape by considerable imperfections. And the current study only considers the case of imperfect mass, but the frequency and mode shape can be derived by adding the stiffness. In addition, it can be applied to ring with circular cross-section as well as cylindrical shell. This paper only consider single mode of tuning but it can do dual mode.

References

[1] W.Soedel, Vibrations of Shells and Plates, Third ed. Marcel Dekker Inc., NY, 2004

[2] Allaei, D., W. Soedel, and T. Y. Yang. Natural frequencies and modes of rings that deviate from perfect axisymmetry. Journal of Sound and Vibration 111.1 (1986): 9-27.

[3] Gardner, Tony G., and C. W. Bert. Vibration of shear deformable rings: theory and experiment. Journal of Sound and Vibration 103.4 (1985): 549-565.

[4] Allaei, D., W. Soedel, and T. Y. Yang. Vibration analysis of non-axisymmetric tires. Journal of sound and vibration 122.1 (1988): 11-29.

[5] Fox, C. H. J. A simple theory for the analysis and correction of frequency splitting in slightly imperfect rings. *Journal of Sound and Vibration* (1990). Vol. 142, Issue 2.

[6] Hong, Jin Sun, and Jang Moo Lee. Vibration of circular rings with local deviation. (1994) : 317-322.

[7] Amabili, Marco. Free vibration of a fluid-filled circular cylindrical shell with lumped masses attached, using the receptance method. Shock and Vibration 3.3 (1996): 159-167.

[8] Park, Yong-Hwa, and Youn-Sik Park. Structure optimization to enhance its natural frequencies based on measured frequency response functions. Journal of Sound and Vibration 229.5 (2000): 1235-1255.

[9] McWilliam, S., J. Ong, and C. H. J. Fox. On the statistics of natural frequency splitting for rings with random mass imperfections. Journal of Sound and Vibration 279.1-2 (2005): 453-470.

[10] Bisegna, P., & Caruso, G. (2007). Frequency split and vibration localization in imperfect rings. *Journal of Sound and Vibration*, *306*(3-5), 691-711.

[11] Gil Park, Han, Yeon June Kang, and Seock Hyun Kim. Dual mode tuning strategy of a slightly asymmetric ring. The Journal of the Acoustical Society of America 123.3 (2008): 1383-1391.

[12] Park, Han Gil, et al. A study on the mode pair of a slightly asymmetric circular ring with multiple deviations. Journal of sound and vibration 310.1-2 (2008): 366-380.

[13] Khoa, Nguyen Viet, and Dao Thi Bich Thao. Theoretical and experimental analysis of the exact receptance function of a clamped-clamped beam with concentrated masses.

Vietnam Journal of Mechanics 42.1 (2020): 29-42.

[14] Tsai, Sung-Han, Huajiang Ouyang, and Jen-Yuan Chang. A receptance-based method for frequency assignment via coupling of subsystems. Archive of Applied Mechanics 90.2 (2020): 449-465.

[15] Zener, Clarence. Internal friction in solids. I. Theory of internal friction in reeds. Physical review 52.3 (1937): 230.

[16] Lifshitz, Ron, and Michael L. Roukes. Thermoelastic damping in micro-and nanomechanical systems. Physical review B 61.8 (2000): 5600.

[17] F.L. Guo, G.A. Rogerson, Thermoelastic coupling effect on a micro-machined beam resonator, Mechanics Research Communications, Vol 30, Issue 6, 2003, Pages 513-518, ISSN 0093-6413,

[18] Wong, S. J., et al. A preliminary investigation of thermo-elastic damping in silicon rings. Journal of micromechanics and micro engineering 14.9 (2004): S108.

[19] Wong, S. J., C. H. J. Fox, and S. McWilliam. Thermoelastic damping of the in-plane vibration of thin silicon rings. Journal of sound and vibration 293.1-2 (2006): 266-285.

[20] K. Tunvir, C.Q. Ru, A. Mioduchowski, Thermoelastic

dissipation of hollow micromechanical resonators, Physica E: Low-dimensional Systems and Nanostructures, Volume 42, Issue 9,

2010, Pages 2341-2352

[21] Pu Li , Hu R. Thermoelastic damping in micromechanical resonators with a proof mass and a network of suspension beams. Japan Society of Applied Physics, 2011, vol 50, 077202

[22] Yong-Chen Pei. Thermoelastic damping in rotating flexible micro-disk. International Journal of Mechanical Sciences 2012;61:52-64.

[23] Parayil, Dileesh V., Salil S. Kulkarni, and Dnyanesh N. Pawaskar. Analytical and numerical solutions for thick beams with thermoelastic damping. International Journal of Mechanical Sciences 94 (2015): 10-19.

[24] Kim JH, Kim JH. Thermoelastic damping effect on the micro-ring resonator with irregular mass and stiffness. Journal of Sound and Vibration 2016; 369: 168-77.

[25] Kim, Sun-Bae, Young-Ho Na, and Ji-Hwan Kim. Thermoelastic damping effect on in-extensional vibration of rotating thin ring. Journal of Sound and vibration 329.9

(2010): 1227-1234.

[26] Kim, Jung-Hwan, and Ji-Hwan Kim. Thermoelastic dissipation of rotating imperfect micro-ring model. International Journal of Mechanical Sciences 119 (2016): 303-309.

[27] Kim, Jung-Hwan, Seok-Joo Kang, and Ji-Hwan Kim. Splitting of quality factors for micro-ring with arbitrary point masses. Journal of Sound and Vibration 395 (2017): 317-327.

[28] Kim, Jung-Hwan, and Ji-Hwan Kim. Mass imperfections in a toroidal micro-ring model with thermoelastic damping. Applied Mathematical Modelling 63 (2018): 405-414.

[29] Kim, Jung-Hwan, and Ji-Hwan Kim. Separation of Q-factors for tubular microstructure with point imperfections. Applied Mathematical Modelling 64 (2018): 572-583.

[30] Rourke, A. K., S. McWilliam, and C. H. J. Fox. Multi-mode trimming of imperfect rings. Journal of Sound and Vibration 248.4 (2001): 695-724.

[31] Rourke. A. K., S. McWilliam, and C.H.J. Fox. Multi-mode trimming of imperfect thin rings using masses at pre-selcted locations. Journal of Sound and Vibration 256.2

(2002) : 319-345

[32] Xi X, Wu X, Zhang Y, Zhou X, Wu X, Wu Y. A study on Q factor of the trimmed resonator for vibratory cupped gyroscopes. Sens Actuators A : Phys 2014;218:23-32

[33] Abdelli, Hamza, Takashiro Tsukamoto, and Shuji Tanaka. Quality factor trimming method using thermoelastic dissipation for multi-ring resonator. Sensors and Actuators A : Physical 332 (2021) : 113044.

Table 1 (a) structural parameter of macro ring

young's modulus, E	$206Gpa$
mass density, μ	$7850kg/m^3$
poisson's ratio, ν	0.3
radius, R	$0.3m$
thickness, h	$0.005m$
length, b	$0.1m$
mass, M_0	$7.3984kg$

Table 1 (b) structural parameter of micro ring

young's modulus, E	$165Gpa$
mass density, μ	$2330kg/m^3$
radius, R	$0.003m$
thickness, h	$120 \times 10^{-6}m$
length, b	$120 \times 10^{-6}m$

Table 2 Thermal properties of temperature

Ambient Temperature T_a $[K]$	258	298	348
Thermal expansion coefficient α $[10^{-6}K^{-1}]$	2.24	2.6	3.06
Heat capacity per unit volume C_v $[10^6 Jm^{-3}K^{-1}]$	1.52	1.64	1.73
Thermal diffusivity χ $[10^{-5}m^2s^{-1}]$	11.7	8.6	6.97

Table 3 (a) Modal frequencies $f_{0n} = \omega_{0n}/(2\pi)$
of the perfect macro−ring

n	2	3	4	5	6
f_{0n} $[Hz]$	36.78	104.03	199.46	322.57	473.21

Table 3 (b) Modal frequencies $f_{0n} = \omega_{0n}/(2\pi)$
of the perfect micro−ring

n	2	3	4	5	6
f_{0n} $[kHz]$	13.83	39.12	75.02	121.32	177.97

Table 4 (a) Modal frequencies of imperfect mass 1%
in macro-ring

	n	2	3	4	5	6
present	H	36.71	103.92	199.35	322.45	473.09
	L	36.49	103.09	197.59	319.48	468.61
ref. [5]	H	36.71	103.92	199.35	322.45	473.09
	L	36.49	103.10	197.61	319.52	468.68

Table 4 (b) Modal frequencies of imperfect mass 1%
in micro-ring without TED

	n	2	3	4	5	6
present	H	13.80	39.09	74.97	121.27	177.92
	L	13.72	38.77	74.31	120.15	176.24
ref. [5]	H	13.80	39.09	74.97	121.27	177.92
	L	13.72	38.78	74.32	120.17	176.27

Table 5 (a) Quality factor of perfect ring with rotating, $\Omega/\omega_{0n} = 0$

n	2	3	4	5	6
T=258K	14444	24164	42125	65144	92817
T=298K	10731	21606	38574	60007	85878
T=348K	7689	16923	30483	47600	68312

Table 5. (b) Quality factor of perfect ring with rotating, $\Omega/\omega_{0n} = 0.5$

	n	2	3	4	5	6
T=258K	forward	18656	26944	42825	62386	85323
	backward	7633	13655	25034	40159	58800
T=298K	forward	13859	24090	39213	57463	78940
	backward	6231	14665	27778	44996	66360
T=348K	forward	9932	18871	30992	45590	62804
	backward	4064	9565	18118	29349	43283

Table 5. (c) Quality factor of perfect ring with rotating, $\Omega/\omega_{0n} = 1$

	n	2	3	4	5	6
T=258K	forward	18489	17402	18665	19286	19544
	backward	1	2	3	4	6
T=298K	forward	13736	15559	17093	17768	18089
	backward	1	3	5	7	11
T=348K	forward	9844	12190	13513	14103	14401
	backward	1	3	5	7	11

Table 6 (a) Quality factor of imperfect mass, $m = 0.01M$ according to the rotating ratio $\Omega/\omega_{0n} = 0$ at T=298K

		$n=2$	$n=3$	$n=4$	$n=5$	$n=6$
present	H	10722	21585	38550	59980	85847
	L	10689	21437	38240	59465	85082
ref[5]	H	10723	21587	38554	59986	85856
	L	10700	21441	38249	59479	85102

Table 6 (b) Quality factor of imperfect mass, $m = 0.01M$ according to the rotating ratio $\Omega/\omega_{0n} = 0.5$ at T=298K

			$n=2$	$n=3$	$n=4$	$n=5$	$n=6$
present	forward	H	13852	24061	39173	57422	78897
		L	13788	23956	38986	57121	78460
	backward	H	5638	12134	22826	36873	54264
		L	5611	12124	22758	36723	54010
ref [5]	forward	H	13853	24067	39186	57436	78911
		L	13833	23887	38798	56785	77939
	backward	H	5655	12187	22899	36965	54375
		L	5610	12012	22532	36351	53456

Table 6 (c) Quality factor of imperfect mass, $m = 0.01M$ according to the rotating ratio $\Omega/\omega_{0n} = 1$ at T=298K

			$n=2$	$n=3$	$n=4$	$n=5$	$n=6$
present	forward	H	13783	15616	17156	17834	18156
		L	13580	15286	16645	17107	17175
	backward	H	1	2	4	6	9
		L	1	2	4	6	9
ref [5]	forward	H	13716	15512	17036	17706	18024
		L	13658	15138	16180	16216	15749
	backward	H	84	189	348	547	779
		L	21	20	19	17	15

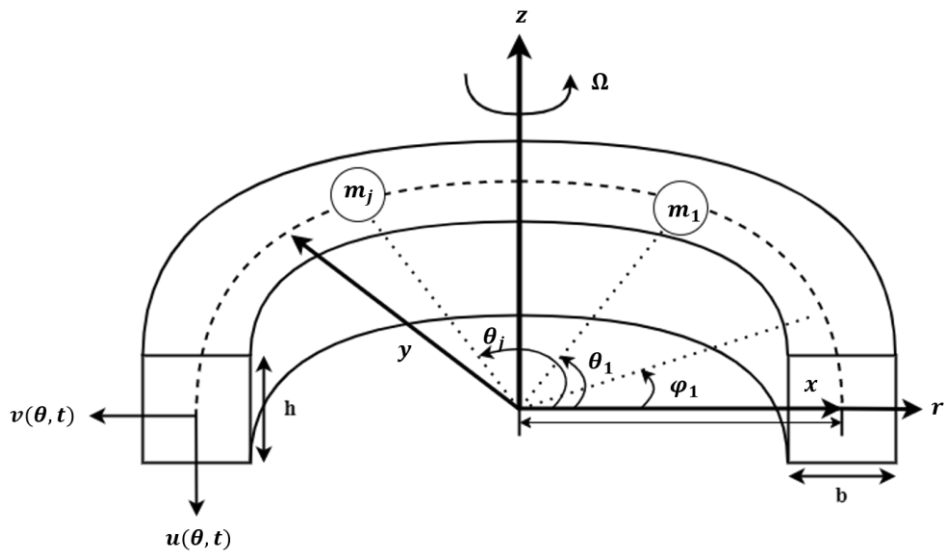

Fig. 1 Coordinate system of ring with imperfections

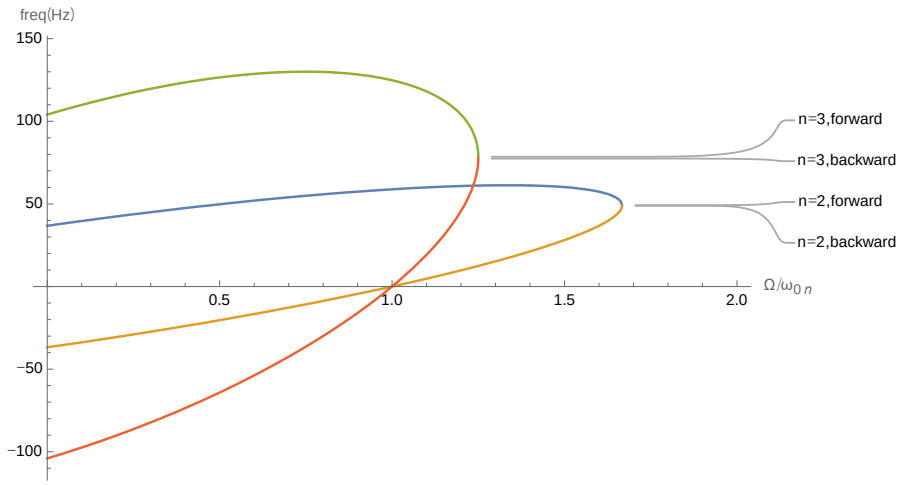

(a) in macro ring

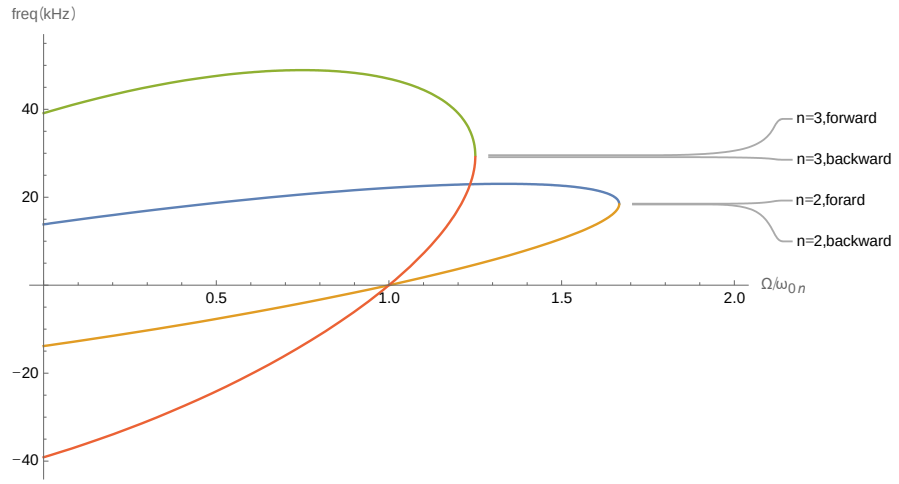

(b) in micro ring without TED

Fig. 2 Modal frequency of perfect ring according to rotating ratio

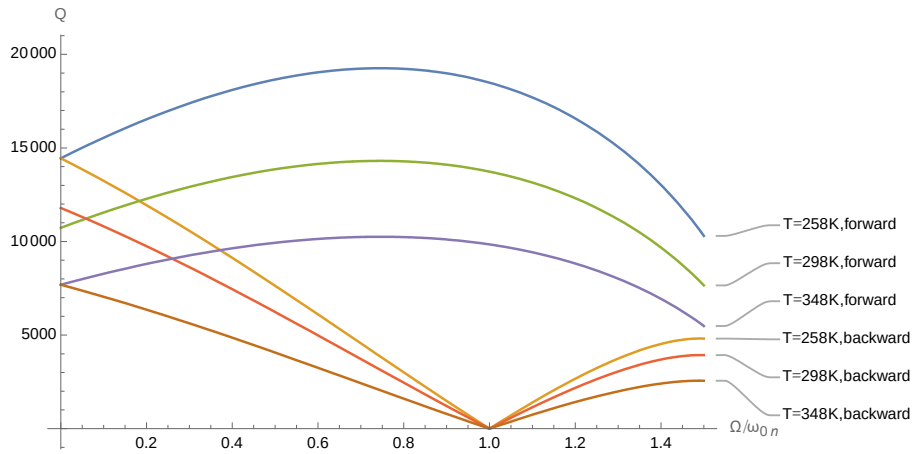

Fig. 3 Q-factor of perfect ring in accordance with rotating speed ratio at n=2

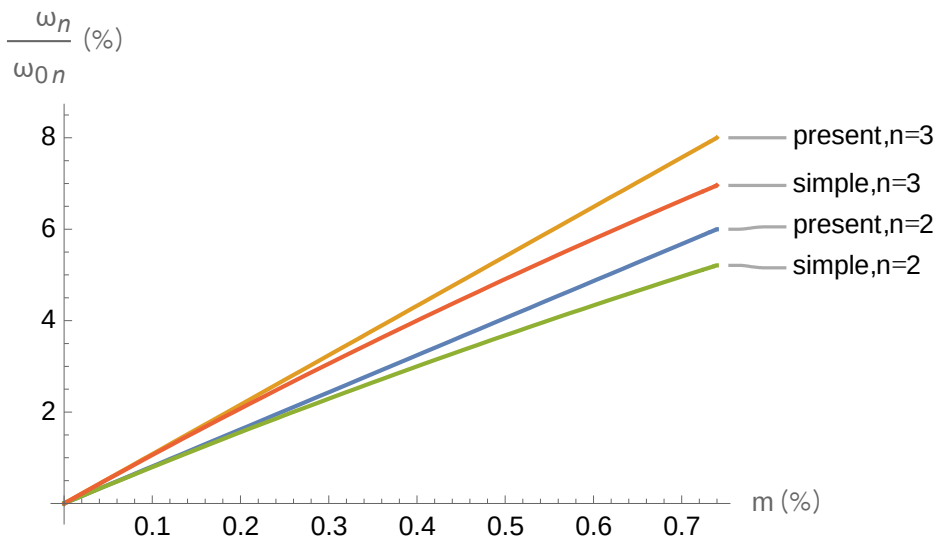

Fig. 4 The difference of higher and lower frequencies in accordance with mass ratio at no rotating

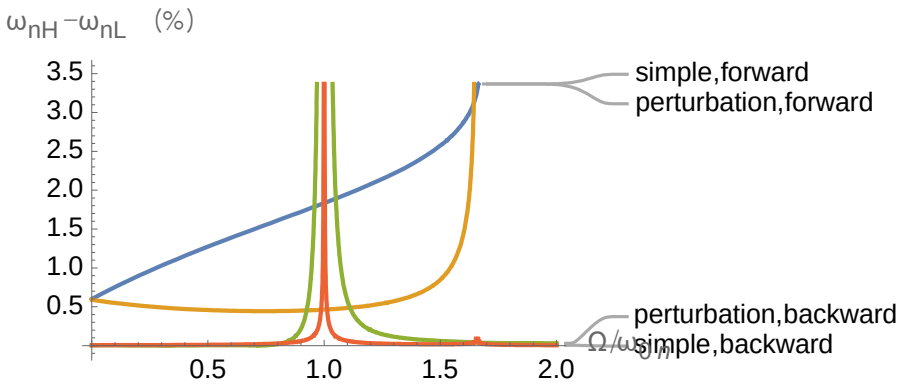

Fig. 5 The difference of higher and lower frequencies in accordance with rotating speed ratio

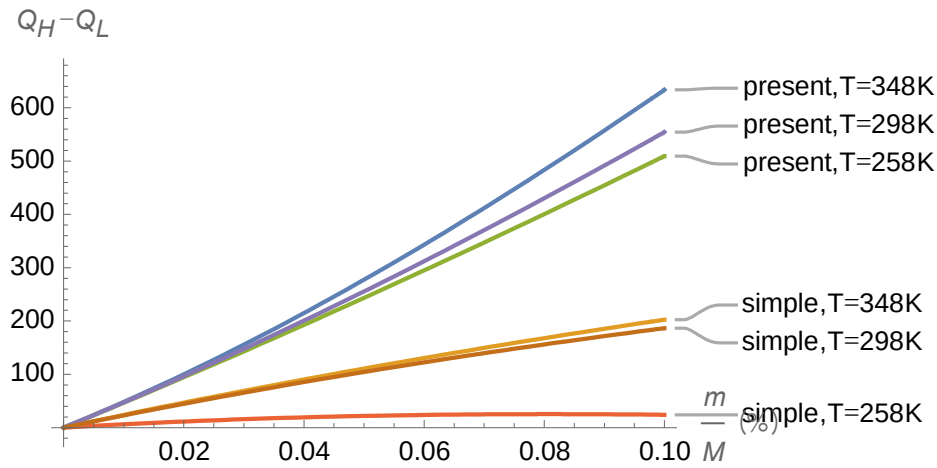

(a) no rotating speed

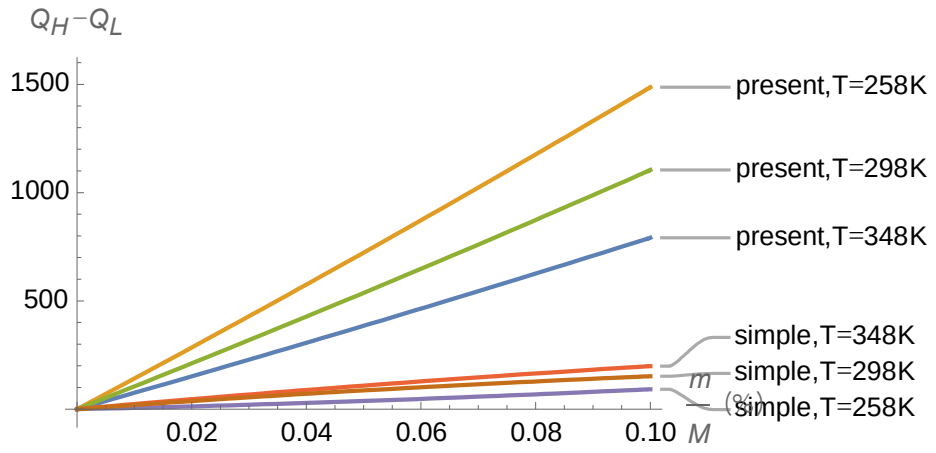

(b) $\Omega/\omega_{0n} = 0.5$

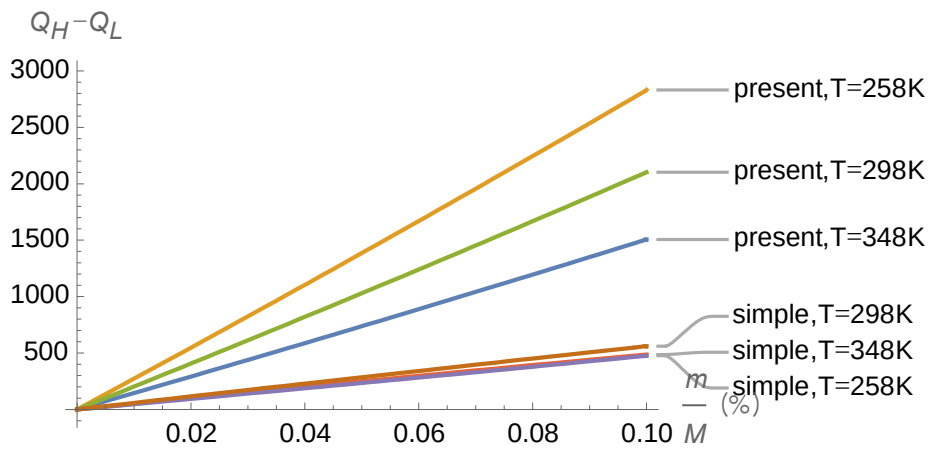

(c) $\Omega/\omega_{0n} = 1$

Fig. 6 The difference of Q−factor according to mass ratio at n=2

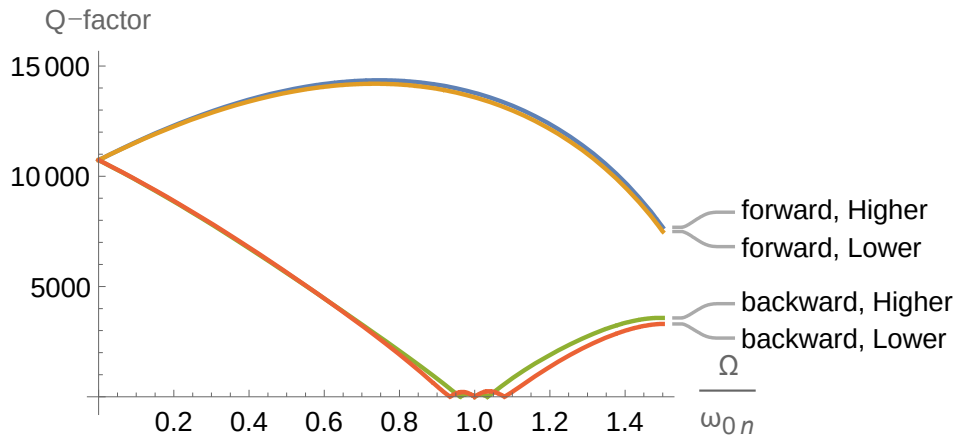

Fig. 7 Q−factor in accordance with rotating speed ratio applied by perturbation at T=298K

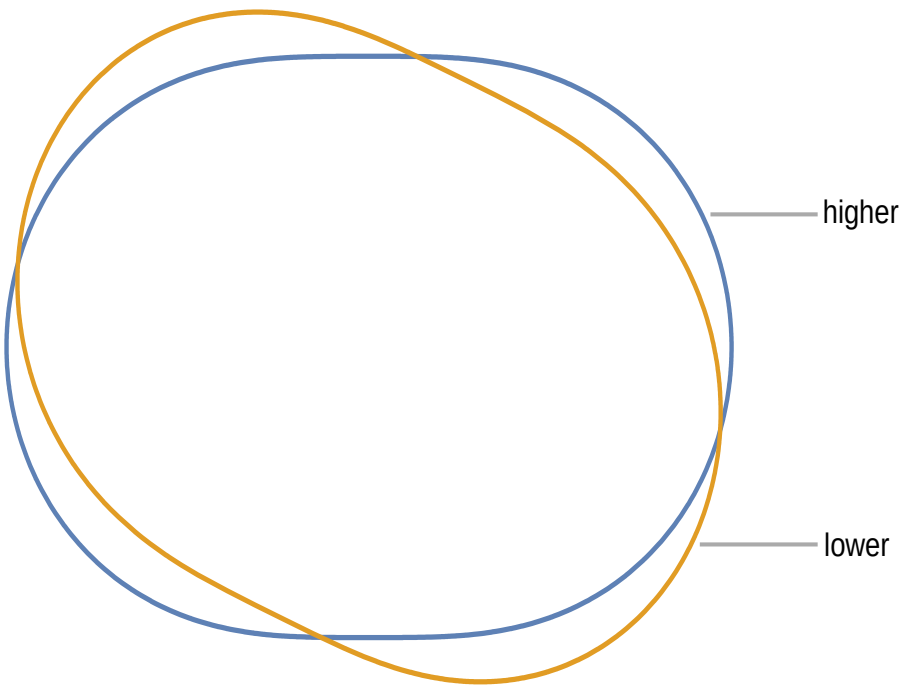

Fig. 8 (a) Mode shape 1% mass with rotating $\Omega/\omega_{0n} = 1$, n=2

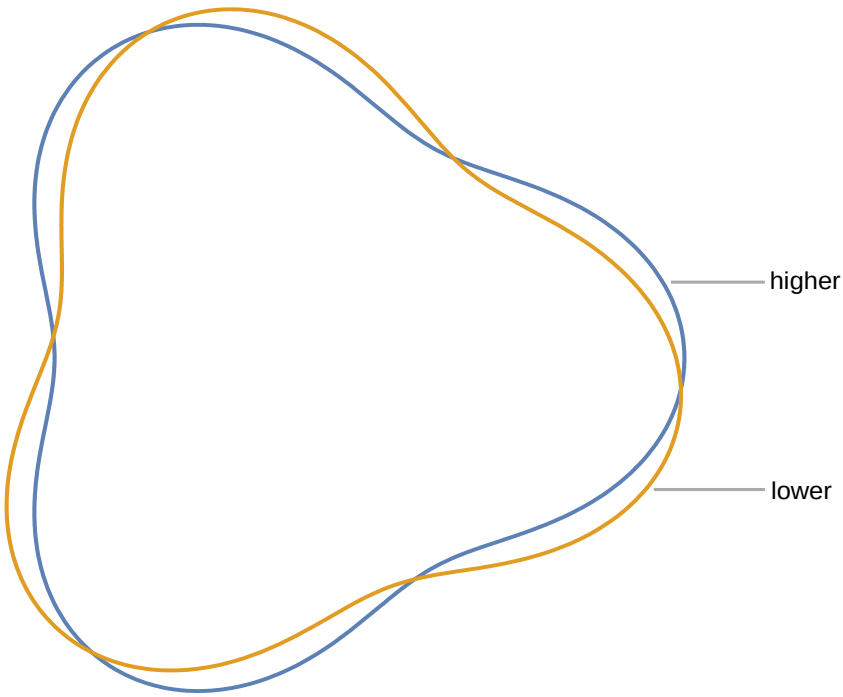

Fig. 8 (b) Mode shape 1% mass with rotating $\Omega/\omega_{0n} = 1$, n=3

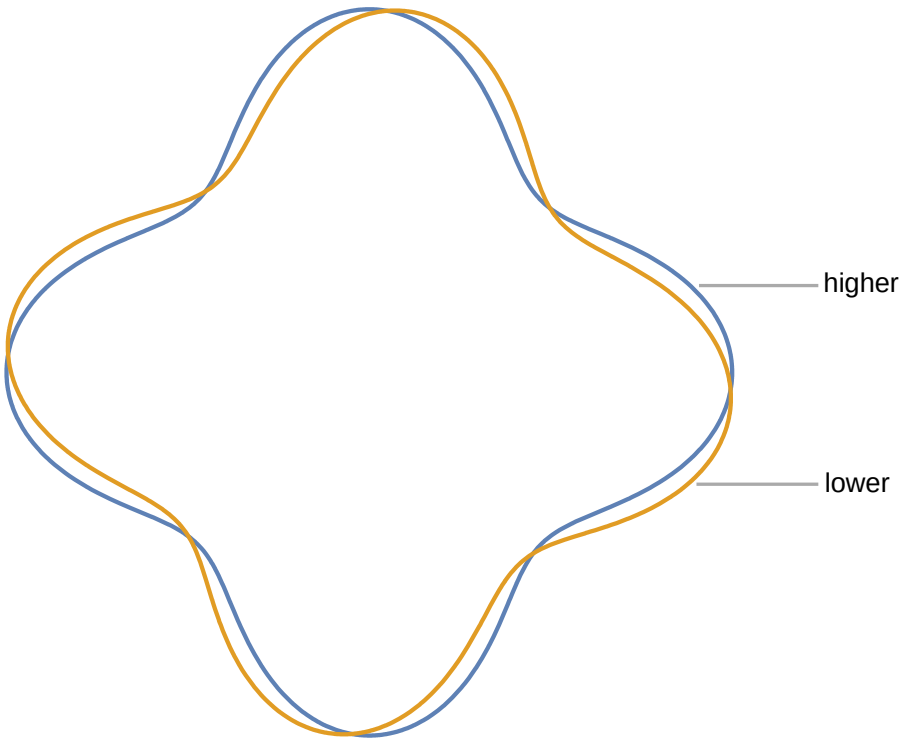

Fig. 8 (c) Mode shape 1% mass with rotating $\Omega/\omega_{0n} = 1$, n=4

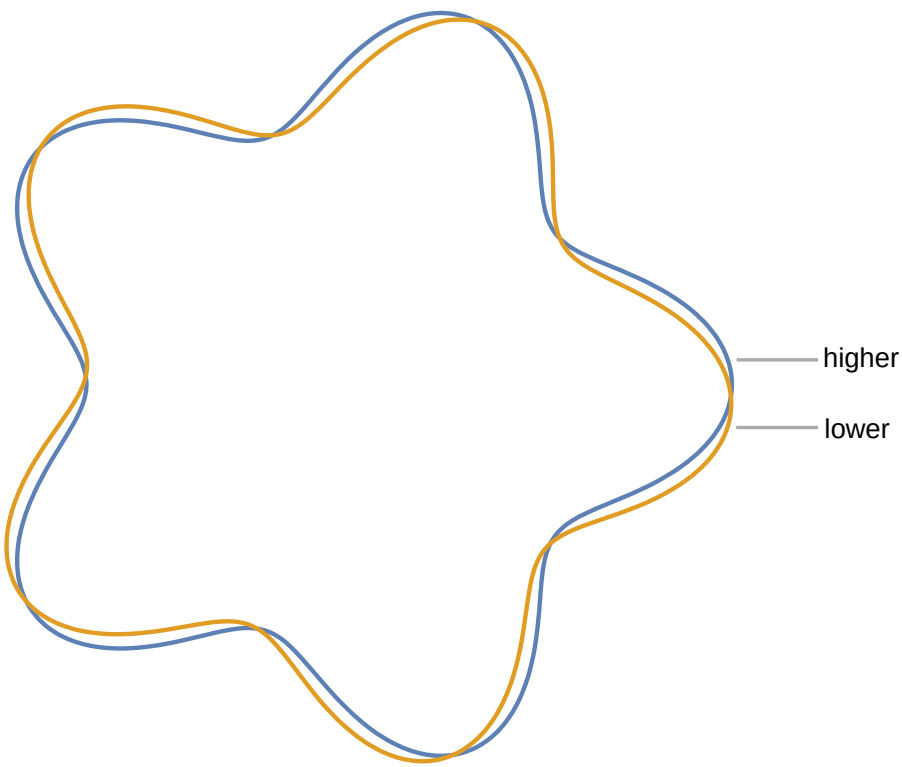

Fig. 8 (d) Mode shape 1% mass with rotating $\Omega/\omega_{0n} = 1$, n=5

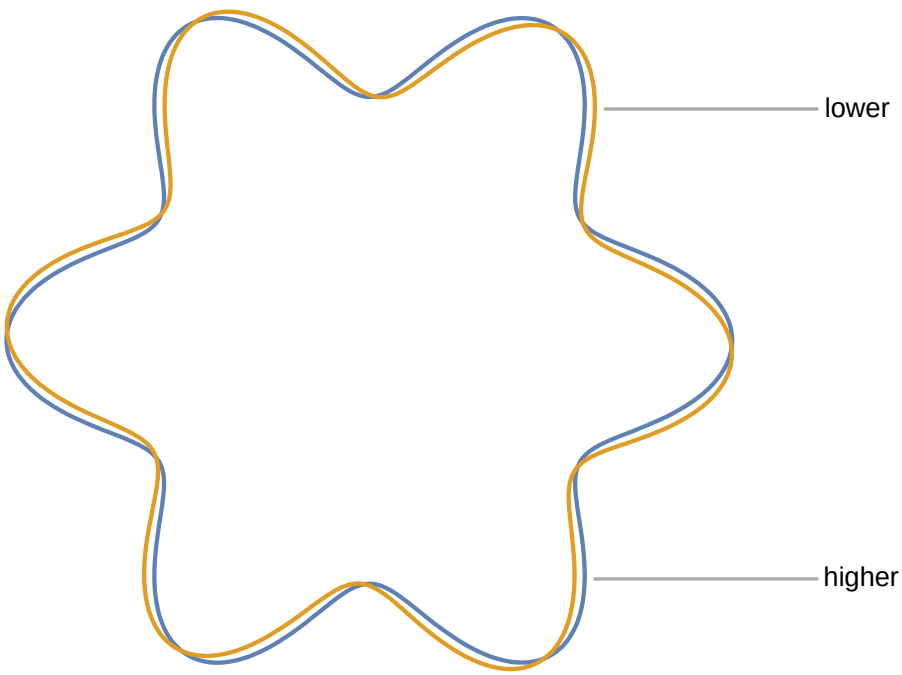

Fig. 8 (e) Mode shape 1% mass with rotating $\Omega/\omega_{0n} = 1$, n=6

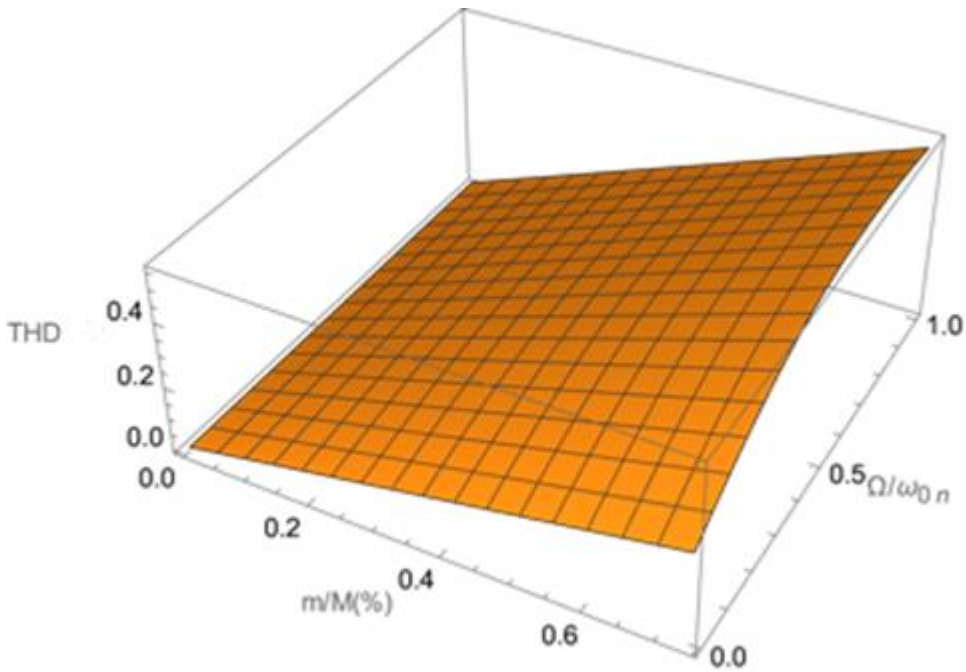

Fig. 9 THD in accordance with mass ratio and rotating speed ratio at n=2 in macro ring

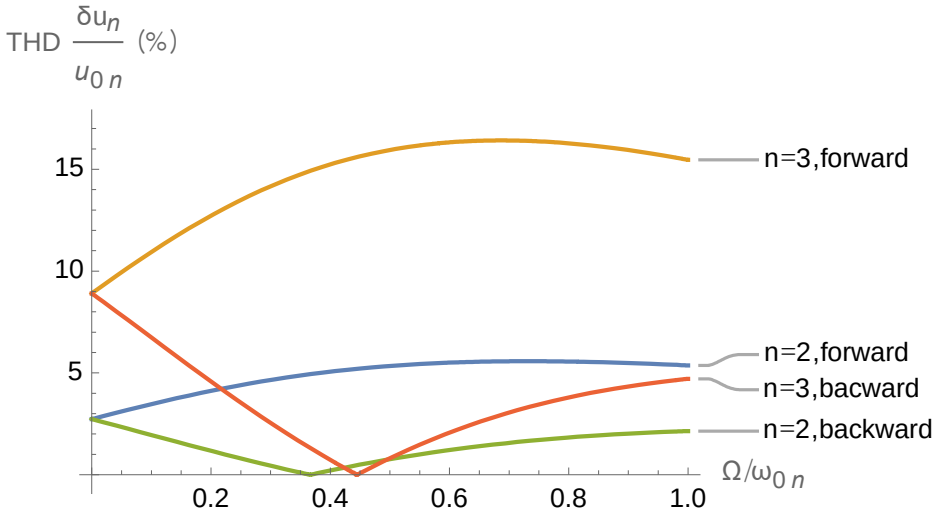

Fig. 10 THD in accordance with rotating speed ratio in micro ring with imperfect mass $\frac{m}{M} = 0.01$

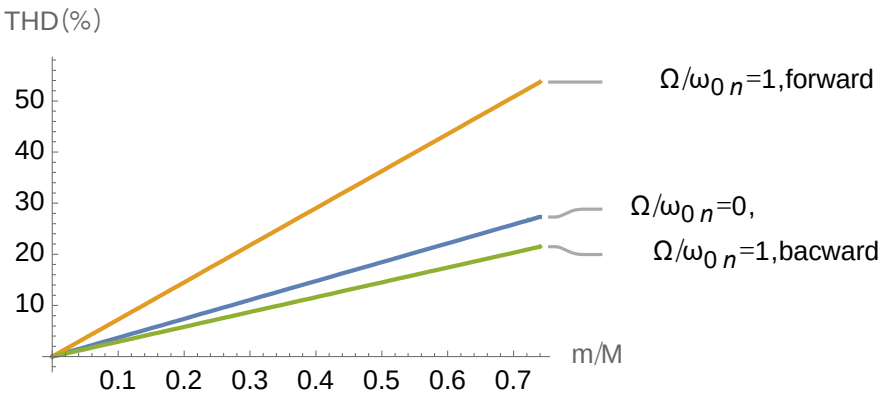

(a) Higher mode

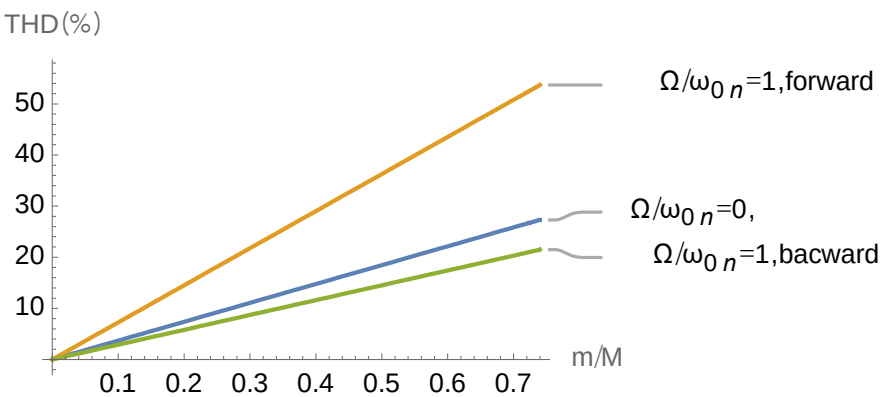

(b) Lower mode

Fig 11. THD in accordance with mass ratio in macro ring

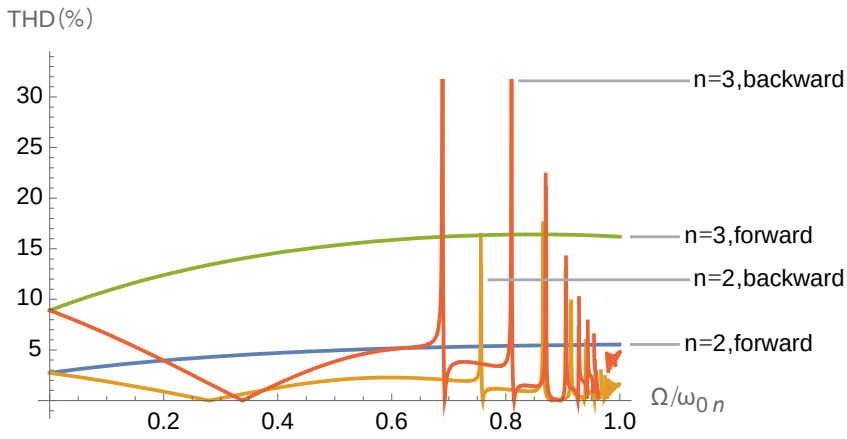

(a) T=258K

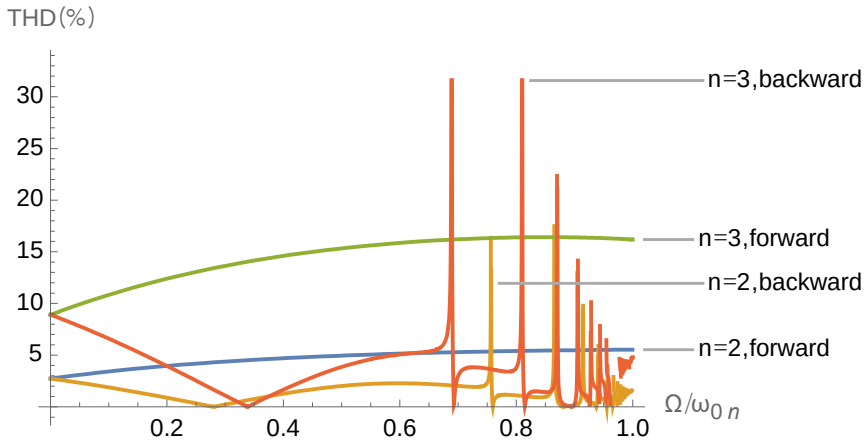

(b) T=298K

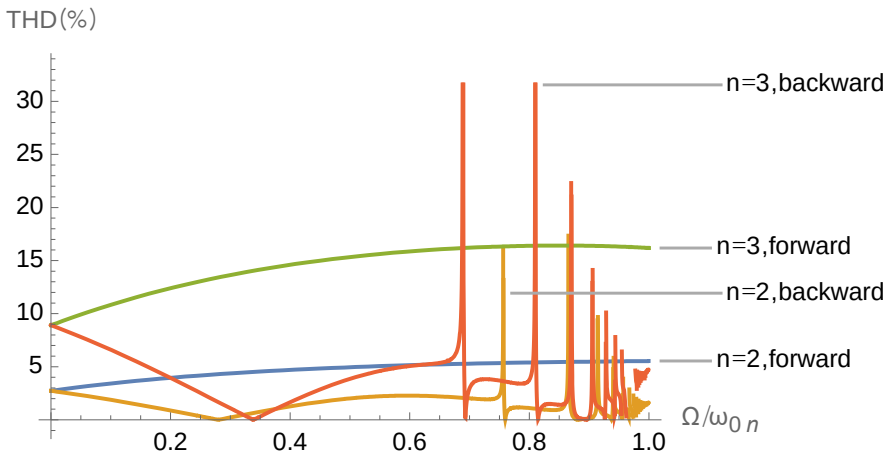

(c) T=348K

Fig. 12 THD in accordance with rotating speed ratio with imperfect mass in micro ring

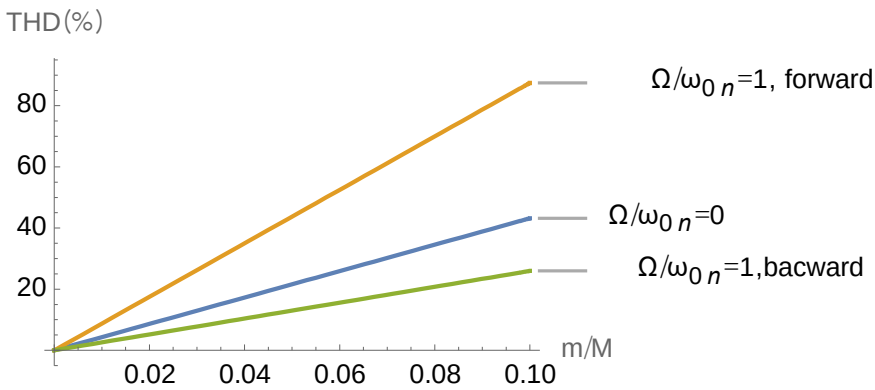

Figure. 13 THD in accordance with mass ratio in micro ring

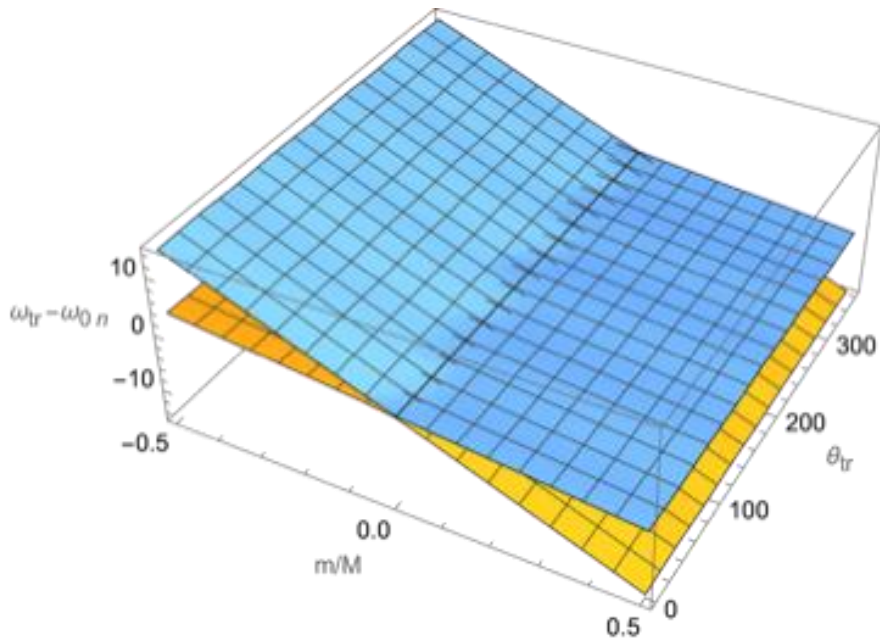

Fig. 14 (a) The difference of frequencies of macro ring in accordance with magnitude and location with trimming mass, $\Omega/\omega_{0n} = 0$, [yellow = Higher mode, blue = Lower mode]

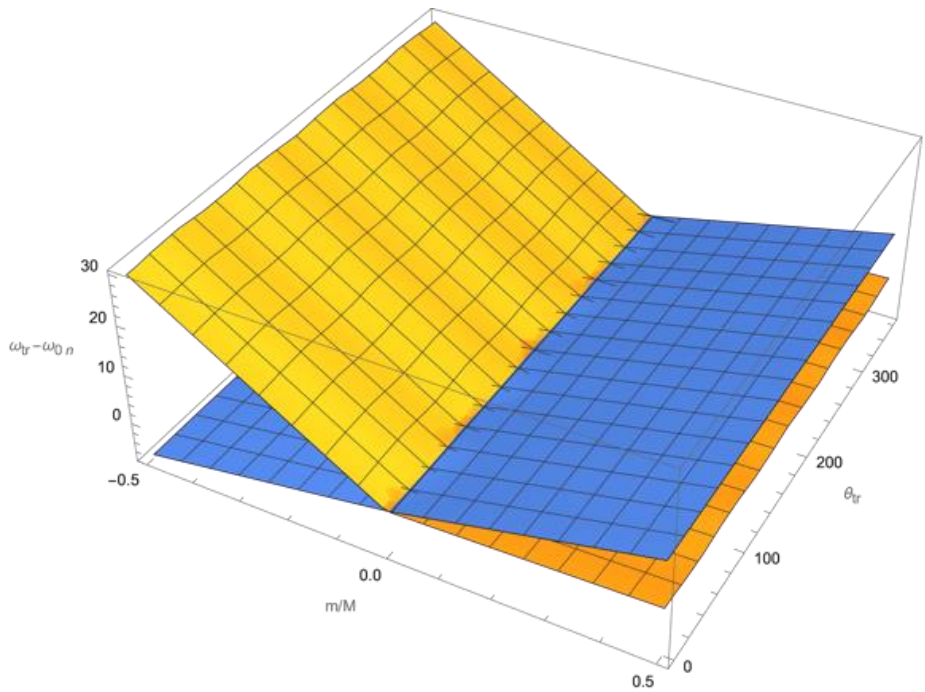

Fig. 14 (b) The difference of frequencies of macro ring in accordance with magnitude and location with trimming mass, $\Omega/\omega_{0n} = 0.5$, [yellow = Higher mode, blue = Lower mode]

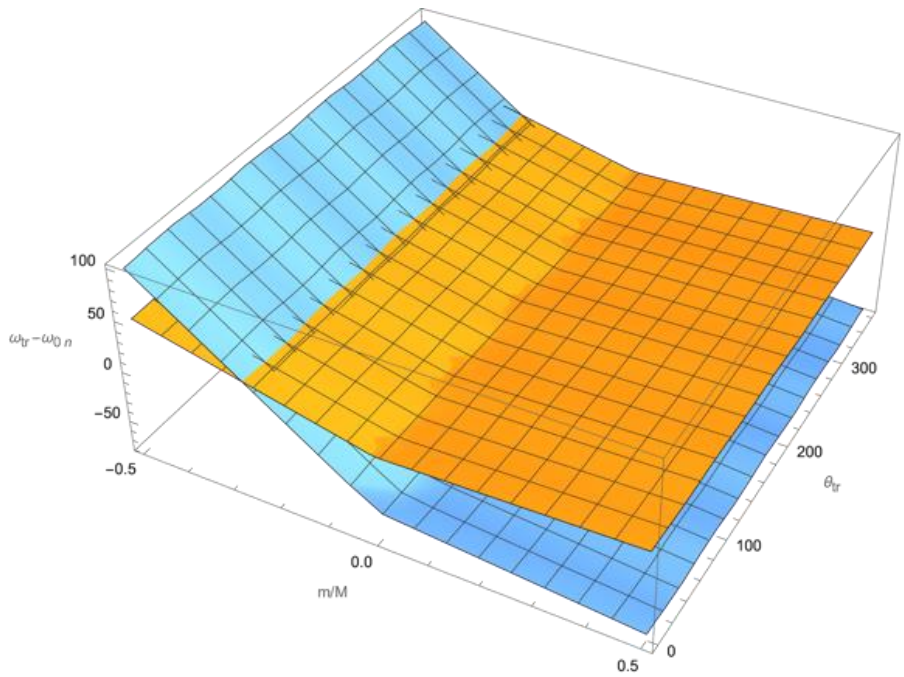

Fig. 14 (c) The difference of frequencies of macro ring in accordance with magnitude and location with trimming mass, $\Omega/\omega_{0n} = 1.1$, [yellow = Higher mode, blue = Lower mode]

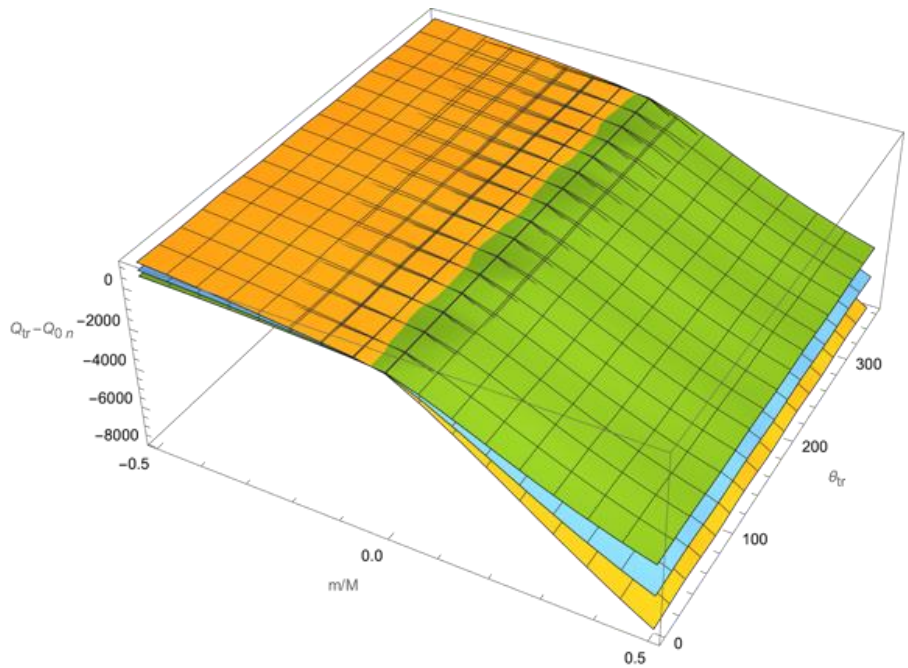

Fig. 15 (a) The difference of quality factor of ring in accordance with magnitude and location with trimming mass, $\Omega/\omega_{0n} = 0$, [yellow = 258K, blue = 298K, green=348K]

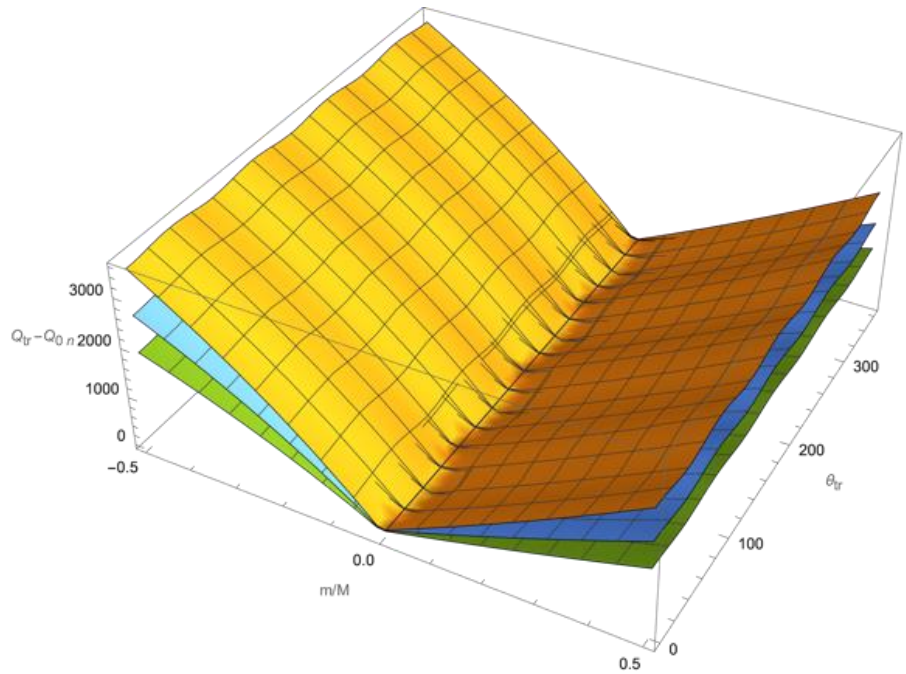

Fig. 15 (b) The difference of quality factor of ring in accordance with magnitude and location with trimming mass, $\Omega/\omega_{0n} = 0.5$, [yellow = 258K, blue = 298K, green=348K]

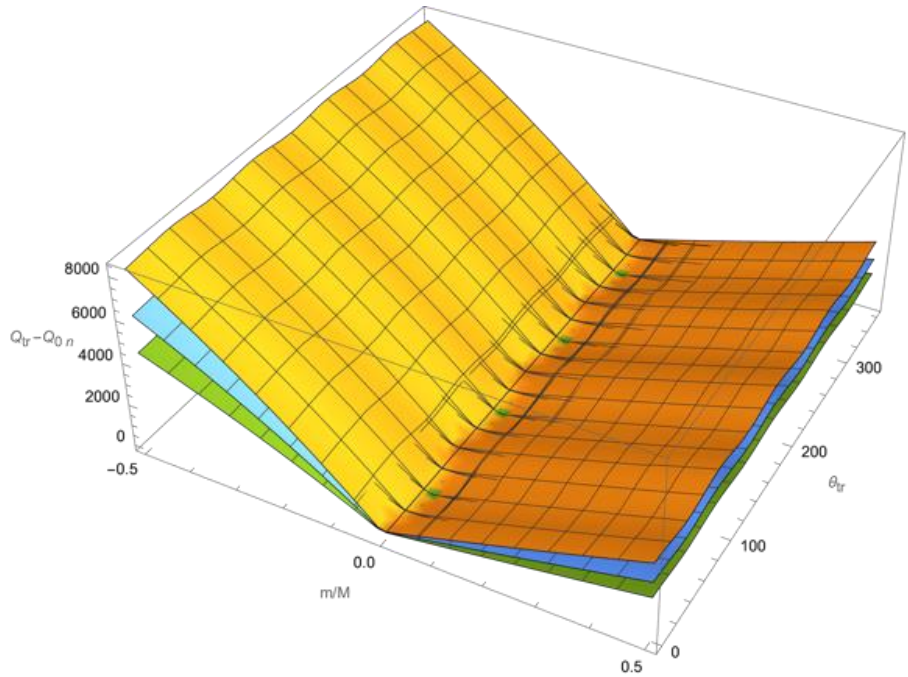

Fig. 15 (c) The difference of quality factor of ring in accordance with magnitude and location with trimming mass, $\Omega/\omega_{0n} = 1$ [yellow = 258K, blue = 298K, green=348K]

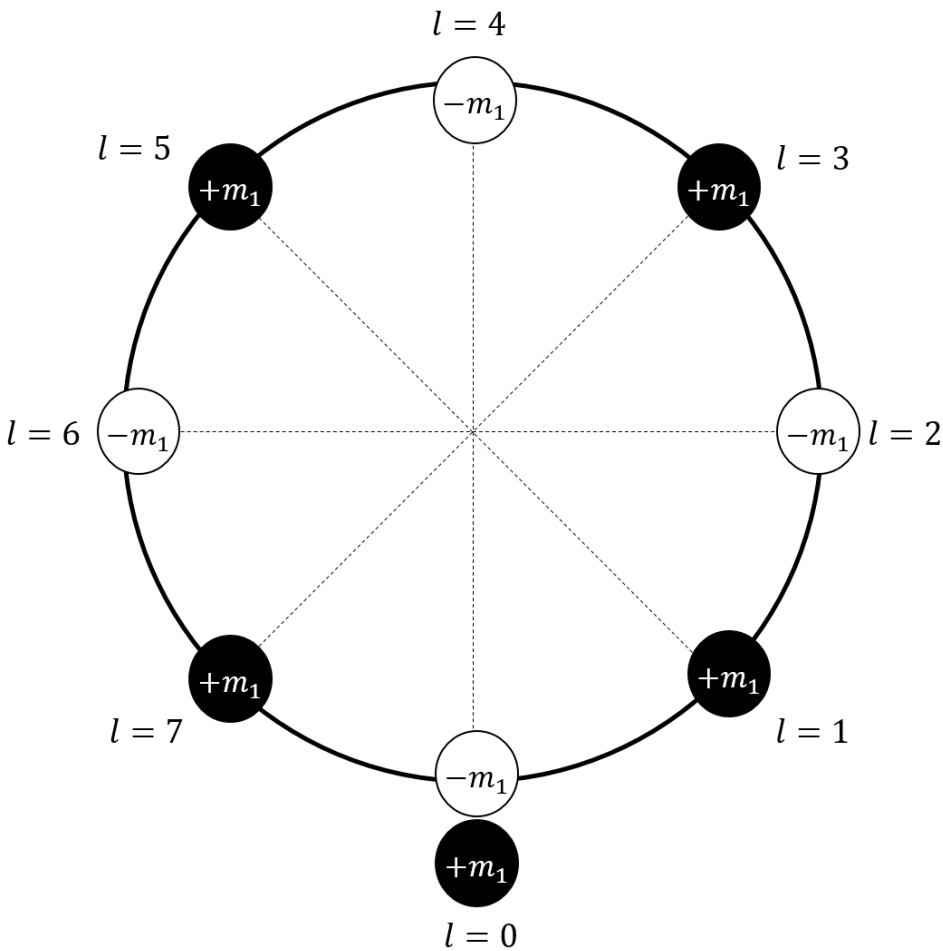

Fig. 16 magnitude and location of tuning mass at n=2

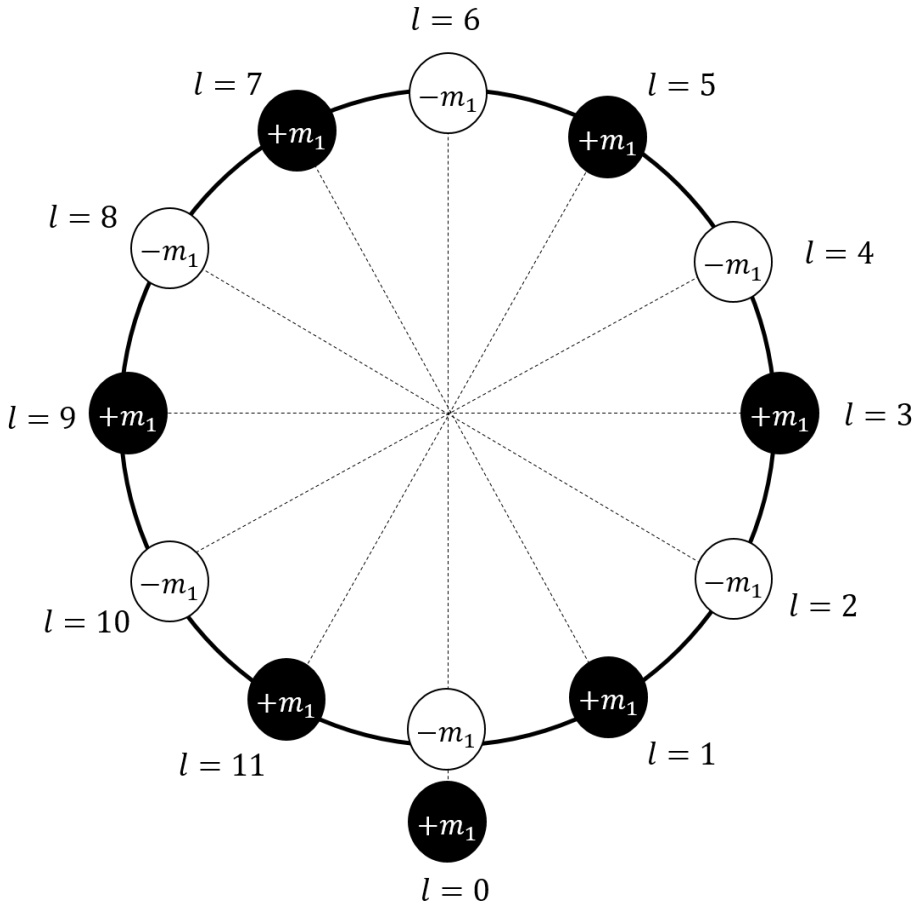

Fig. 17 magnitude and location of tuning mass at n=3

국 문 초 록

많은 구조물들은 완벽하게 설계 및 디자인을 하여 제작한다. 그러나 실제로는 몇몇의 불안정성 때문에 완전한 구조물에 영향을 끼친다. 또한, 시간이 지남으로써 무게가 떨어지거나 단면적 또는 부피의 변형으로 인해 구조물의 진동이 달라진다. 그래서 구조물 불안전성에 대한 진동을 예측하기 위해서는 식 전개과정에서 같이 고려해서 계산해야한다. 그리고 회전속도비가 구조물의 주파수와 모드 형상에 영향을 끼친다. 그래서 Receptance 방법을 사용하여 질량에 의한 불안정 구조물이 회전하고 있는 상황에서 불안정한 질량에 의해 갈라지는 주파수 증가량을 구하여 simple theory와 비교한다. 더 나아가, simple theory에서 못 구하는 모드 형상을 구해 모드 형상 변화값을 계산한다. 특히, 회전 속도 비에 의해서도 전진 회전 주파수와 후진 회전 주파수로 나누어진다. 후진 회전 주파수에서 회전하고 있는데 주파수가 없는 상황인 정지 상태를 볼 수 있다. 마이크로 구조물에서는 주파수 뿐만 아니라 성질 계수가 중요한데 receptance로 구한 주파수로 열탄성 감폭 효과를 적용시켜 마이크로에서의 성질 계수를 계산 할 수 있다. 마찬가지로, 불안정한 질량에 의해 주파수와 같이 성질 계수도 갈라진다. 불안정한 구조물을 안정한 구조물로 만들 수 있는 방법을 알아내기 위해 불안정한 구조물의 주파수를 구한 과정을 역으로 도출한다. 그래서 불안정한 구조물로 인해 갈라지 주파수를 다시 합치거나 없앨 수 있는 새로운

질량의 무게와 위치를 계산할 수 있는 과정을 제시한다.

주요어 : 불안정 질량, 스플릿, 열탄성 감폭 효과, 성질 계수, 마이크로링

학 번 : 2021-26006